Geomorphology 370 (2020) 107369

Contents lists available at ScienceDirect

Geomorphology

journal homepage: www.elsevier.com/locate/geomorph

Morphometry of bedrock meltwater channels on Antarctic inner continental shelves: Implications for channel development and subglacial hydrology

James D. Kirkham [a,b,*], Kelly A. Hogan [b], Robert D. Larter [b], Neil S. Arnold [a], Frank O. Nitsche [c], Gerhard Kuhn [d], Karsten Gohl [d], John B. Anderson [e], Julian A. Dowdeswell [a]

[a] Scott Polar Research Institute, University of Cambridge, Cambridge CB2 1ER, UK
[b] British Antarctic Survey, Natural Environment Research Council, Cambridge CB3 0ET, UK
[c] Lamont-Doherty Earth Observatory of Columbia University, New York, NY 10964-8000, USA
[d] Alfred Wegener Institute, Helmholtz Centre for Polar and Marine Research, 27568 Bremerhaven, Germany
[e] Department of Earth Sciences, Rice University, Houston, TX 77005, USA

ARTICLE INFO

Article history:
Received 19 May 2020
Received in revised form 4 August 2020
Accepted 4 August 2020
Available online 8 August 2020

Keywords:
Subglacial meltwater channels
Antarctica
Continental shelf
Morphometry
Subglacial lakes
Paleoglaciology

ABSTRACT

Expanding multibeam bathymetric data coverage over the last two decades has revealed extensive networks of submarine channels incised into bedrock on the Antarctic inner continental shelf. The large dimensions and prevalence of the channels implies the presence of an active subglacial hydrological system beneath the past Antarctic Ice Sheet which we can use to learn more about inaccessible subglacial processes. Here, we map and analyse over 2700 bedrock channels situated across >100,000 km^2 of continental shelf in the western Antarctic Peninsula and Amundsen Sea to produce the first inventory of submarine channels on the Antarctic inner continental shelf. Morphometric analysis reveals highly similar distributions of channel widths, depths, cross-sectional areas and geometric properties, with subtle differences between channels in the western Antarctic Peninsula compared to those in the Amundsen Sea. At 75–3400 m wide, 3–280 m deep, 160–290,000 m^2 in cross-sectional area, and typically 8 times as wide as they are deep, the channels have similar morphologies to tunnel valleys and meltwater channel systems observed from other formerly glaciated landscapes despite differences in substrate geology and glaciological regime. We propose that the Antarctic bedrock channels formed over multiple glacial cycles through the episodic drainage of at least 59 former subglacial lakes identified on the inner continental shelf.

1. Introduction

The distribution and flux of subglacial water is a fundamental modulator of ice-sheet dynamics (Bell, 2008). The presence of an efficient channelised drainage system can increase basal shear stresses, drive up effective pressures, and reduce ice-flow velocities (Schoof, 2010; Hewitt, 2013). Conversely, elevated pore water pressures, resulting from the inefficient evacuation of subglacial meltwater from the bed of an ice sheet, may reduce effective basal pressures, facilitating fast-ice flow (Anandakrishnan et al., 1998; Tulaczyk et al., 2000; Peters et al., 2006). Understanding the manner in which subglacial water flows beneath ice sheets, and its implications for ice-sheet velocities and ice dynamics, is thus critical to the accurate prediction of future ice-sheet behaviour, and for the interpretation of geomorphological evidence of former ice-flow patterns preserved in the palaeo-record.

The subglacial water present beneath an ice sheet can be derived from several sources: surface meltwater that drains to the bed (e.g. Das et al., 2008; Bartholomew et al., 2012), basal melting of ice through geothermal or frictional strain heating (e.g. Pattyn, 2010; Dowdeswell et al., 2016), and water influx from underlying aquifers (e.g. Boulton et al., 1995; Piotrowski, 1997; Christoffersen et al., 2014). With the exception of the Antarctic Peninsula and the ice shelves that fringe the continent (Trusel et al., 2013; Bell et al., 2017, 2018; Kingslake et al., 2017), the polar desert climate characterising the majority of the contemporary Antarctic Ice Sheet largely prevents the production of surface meltwater. Consequently, the water present within the Antarctic subglacial hydrological system is sourced mainly from processes that occur at the ice-sheet bed (Rose et al., 2014). However, whilst the absence of surface melting limits the quantity of meltwater available, the Antarctic subglacial hydrological system remains a major influence on ice-sheet dynamics and mass-loss rates (Nitsche et al., 2013; Dowdeswell et al., 2016).

* Corresponding author at: British Antarctic Survey, Natural Environment Research Council, Cambridge CB3 0ET, UK.
E-mail address: jk675@cam.ac.uk (J.D. Kirkham).

https://doi.org/10.1016/j.geomorph.2020.107369

Low hydraulic-potential gradients at the base of the Antarctic Ice Sheet facilitate extensive water ponding, producing subglacial lakes in regions of hydraulic potential minima (Robin et al., 1970; Oswald and Robin, 1973; Siegert et al., 1996, 2005, 2016; Wright and Siegert, 2011; Willis et al., 2016). A number of Antarctic subglacial lakes have been observed to drain over several months, issuing pulses of accumulated subglacial meltwater that are routed several hundred kilometres through the Antarctic subglacial hydrological system (e.g. Wingham et al., 2006; Fricker et al., 2007; Flament et al., 2014). Subglacial lakes are commonly documented upstream of ice-stream onset zones, suggesting that this could be a mechanism that initiates the high flow velocities associated with streaming ice (Siegert and Bamber, 2000). Changes in the routing of Antarctic subglacial meltwater have also been associated with dynamic ice-flow behaviour including the acceleration, deceleration, and on-off switching of the Siple Coast ice streams in the Ross Embayment (Alley et al., 1994; Jacobel et al., 2000; Anandakrishnan et al., 2001; Joughin et al., 2002). Furthermore, at Byrd Glacier, ice velocity has been observed to increase during a subglacial lake drainage event (Stearns et al., 2008).

In addition to influencing ice-sheet movement, the expulsion of subglacial water from the Antarctic Ice Sheet has broad implications for global climate and, through feedbacks, could lead to enhanced ice-sheet and ice-shelf melting (Bronselaer et al., 2018). Recent work has established a link between the routing and expulsion of meltwater from beneath the contemporary ice sheet and increased rates of ice-shelf melting (e.g. Wei et al., 2020). Meltwater expelled from channels beneath the Antarctic Ice Sheet initiates convective cells which carry warm ocean water to the underside of ice shelves, resulting in enhanced melt rates (Jenkins, 2011; Le Brocq et al., 2013; Wei et al., 2020). Material released by these sediment-laden meltwater plumes has been deposited as a fine-grained sediment drape offshore of the margin of the West Antarctic Ice Sheet as it retreated over the last 7–8 kyr, indicating that ice-sheet retreat has coincided with abundant meltwater activity in the past (Kirshner et al., 2012; Witus et al., 2014).

Geophysical evidence suggests the presence of active drainage networks beneath the contemporary Antarctic Ice Sheet which have important implications for ice-sheet dynamics and mass loss (e.g. Wingham et al., 2006; Fricker et al., 2007; Schroeder et al., 2013; Wei et al., 2020). However, the vast extent and thickness of the Antarctic Ice Sheet limits our ability to obtain high-resolution observations of contemporary subglacial drainage processes. This issue is exacerbated by the fact that many subglacial processes operate over timescales that are longer than currently covered by the length of contemporary glaciological observations, such as the multi-decadal to centennial recurrence intervals estimated for subglacial lake drainage (Willis et al., 2016). Consequently, the exact nature of the Antarctic subglacial hydrological system is still not fully resolved (Lowe and Anderson, 2003; Ashmore and Bingham, 2014).

Examining the marine record of subglacial landforms produced by former glaciations and preserved on the seafloor offers an alternative means of investigating ice-sheet beds (e.g. Dowdeswell et al., 2016). This approach has the advantage of capturing the imprints of glacial processes that occur over both short and long timescales, whilst the lack of ice cover permits high-resolution mapping to be conducted without obstruction or loss of detail. The inner continental shelves of many formerly glaciated high-latitude continental margins have been extensively scoured by glacial erosion, producing deep cross-shelf troughs that funnelled ice flow towards the continental-shelf break during full glacial conditions (Anderson et al., 2002; Evans et al., 2009; Larter et al., 2009; Jakobsson et al., 2012; Livingstone et al., 2012; Dowdeswell et al., 2014; Batchelor and Dowdeswell, 2014). Subglacial bedforms develop under specific conditions at the ice-bed interface, so the presence and distribution of submarine glacial landforms within cross-shelf troughs can be used to reconstruct the velocity structure, basal processes and retreat chronology of past ice sheets (Stokes and Clark, 2002; Dowdeswell et al., 2016).

Lowe and Anderson (2002, 2003) were among the first to identify channel features on the Antarctic continental shelf. Technological advances in the resolution and processing of multibeam echosounder data (Jakobsson et al., 2016), combined with the increasing spatial coverage of multibeam surveys, have revealed that channels are abundant on the largely bedrock-dominated inner continental shelves of the western Antarctic Peninsula (e.g. Ó Cofaigh et al., 2002, 2005; Domack et al., 2006; Anderson and Oakes-Fretwell, 2008; Larter et al., 2019) and West Antarctica (e.g. Lowe and Anderson, 2003; Larter et al., 2009; Nitsche et al., 2013; Kirkham et al., 2019). The bedrock channels are typically kilometres in width, several hundred metres deep and possess undulating thalwegs that indicate erosion by pressurised subglacial meltwater (Lowe and Anderson, 2002). The widespread distribution and extensive dimensions of the bedrock channels implies that substantial quantities of subglacial water were present during their formation. However, numerical calculations show that an abundance of meltwater is inconsistent with the low basal melt rates produced by geothermal and strain heating beneath the majority of the Antarctic Ice Sheet (e.g. Perol et al., 2015; Martos et al., 2017; Bougamont et al., 2019), raising the question of how such large channels could have been eroded into bedrock to the scales observed on the Antarctic continental shelf (Nitsche et al., 2013; Rose et al., 2014). The processes responsible for the Antarctic channel systems thus remain unresolved.

Although channels have been observed extensively across several regions of the Antarctic inner-continental shelf, a rigorous quantitative analysis of channel morphometry is lacking. Consequently, the extent to which different channelised regions of the Antarctic continental shelf share comparable physical properties, and thus a potentially similar formative mechanism, remains unconstrained. Improving our understanding of these landforms and how they formed will ultimately inform our knowledge of Antarctic subglacial hydrology, and advance our ability to accurately represent these processes in numerical ice-sheet models. This work aims to utilise the now extensive multibeam bathymetric datasets on the Antarctic continental shelf to: (i) analyse the morphometry of the bedrock channels present in this region; and to (ii) investigate links to subglacial hydrological processes, which are inaccessible beneath the present-day ice sheet bed and may not have been captured by contemporary glaciological observations. We produce the first comprehensive quantitative inventory of Antarctic submarine channelised landforms, documenting >2700 bedrock channels situated on over 100,000 km^2 of the Antarctic inner continental shelf. The morphology of the channels is examined quantitatively and the characteristics of four different channelised regions in the western Antarctic Peninsula and the Amundsen Sea are compared.

2. Regional setting

The study area extends from the western Antarctic Peninsula to the western Amundsen Sea Embayment, spanning latitudes of ~64°S to ~75°S (Fig. 1). Glaciers along this margin, particularly those in the Amundsen Sea Embayment, are currently accelerating and retreating rapidly due to oceanic intrusions of warm Circumpolar Deep Water towards their grounding lines (e.g. Jacobs et al., 1996; Jenkins et al., 1997, 2010; Hillenbrand et al., 2017; Rignot et al., 2019). The continental shelf in this region is relatively broad and extends over 400 km from the contemporary ice margin; this served as a platform for ice sheets to expand and retreat across during previous full-glacial periods (e.g. Larter and Barker, 1989; Larter and Cunningham, 1993; Bart and Anderson, 1995; Domack et al., 2006; Lowe and Anderson, 2003; Graham et al., 2009; Larter et al., 2014). Present-day water depths locally exceed 1600 m on the inner continental shelf, which is generally composed of crystalline bedrock exposed at the seafloor (e.g. Gohl et al., 2013). In contrast, the outer shelf is made up of prograding sedimentary strata overlain by recent sediments and is characterised by shallower water depths in the range of ~400–600 m (Larter and Barker, 1989; Nitsche et al., 2007).

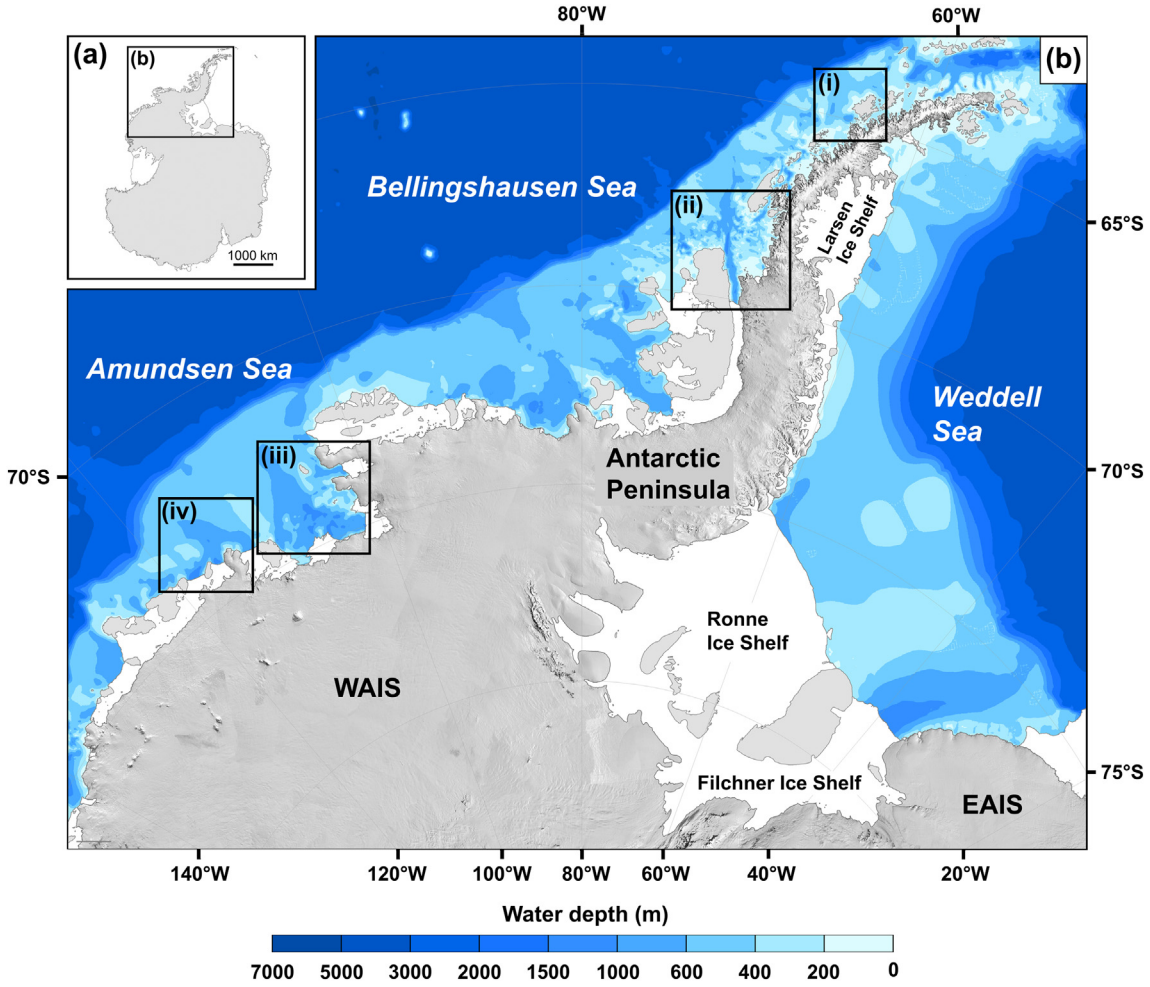

Fig. 1. Study locations. (a) Map of Antarctica displaying the region examined in this study. (b) Regional bathymetry of the western Antarctic Peninsula and the Amundsen, Bellingshausen and Weddell seas displaying the locations of the four areas surveyed by detailed multibeam bathymetry: (i) Anvers-Hugo Trough, (ii) Marguerite Bay, (iii) Pine Island Bay, and (iv) offshore of the Dotson-Getz ice shelves. The Antarctic continent is displayed as a shaded Landsat Image Mosaic of Antarctica (U.S. Geological Survey, 2007). Regional bathymetry is derived from the International Bathymetric Chart of the Southern Ocean (IBCSO) (Arndt et al., 2013). WAIS refers to the West Antarctic Ice Sheet; EAIS refers to the East Antarctic Ice Sheet.

The present continental shelf has been sculpted by numerous glaciations, resulting in a gross morphology that consists of a series of shallower banks separated by broad, deep U-shaped troughs that were eroded by fast-flowing ice streams (e.g. Rebesco et al., 1998; Nitsche et al., 2007; Graham et al., 2010). Evidence for multiple glacial advances is recorded in the thick sedimentary sequences on the outer continental shelf which contain unconformity surfaces scoured by glacial erosion — these have been retrieved through ocean drilling projects and dated using diatom and radiolarian biostratigraphy to constrain the timing of former glacial occupation of the shelf (e.g. Bart and Anderson, 1995; Larter and Barker, 1989; Larter and Cunningham, 1993; Bart, 2001; Barker and Camerlenghi, 2002; Bart et al., 2005). These data reveal that grounded ice sheets first flowed onto the western Antarctic Peninsula continental shelf during the middle or late Miocene (between ~14 and 8 Ma). Repeated advances of grounded ice across the continental shelf from the late Miocene to early Pliocene mark the inception of a fully glaciated margin in this area between 8 and 5 Ma (Bart, 2003; Chow and Bart, 2003; Bart et al., 2005; Hernández-Molina et al., 2017). Similarly, erosional unconformities in the Amundsen Sea have been tentatively correlated with drill sites in the Ross Sea, leading to the inference that grounded ice first advanced onto the middle shelf of the Amundsen Sea Embayment during the middle Miocene (Gohl et al., 2013; Lindeque et al., 2016). The presence of numerous unconformities in the younger part of the geological record has been interpreted as evidence of more frequent advances and retreats of grounded ice beginning in the late Miocene and continuing into the Pliocene and Pleistocene in this area (Gohl et al., 2013). The most recent period of grounded ice advance and retreat across the continental shelf is documented through the presence of glacial landforms at the base of the cross-shelf troughs including drumlins, mega-scale glacial lineations and grounding-zone wedges. These landforms demonstrate that a grounded ice sheet expanded across the middle and outer continental shelf during the Last Glacial Maximum (23–19 cal ka BP) before retreating relatively synchronously across the different ice sheet sectors from the Antarctic Peninsula to the Amundsen Sea, including a phase of rapid retreat close to the modern ice margins which finished prior to 10,000 years ago (e.g. Ó Cofaigh et al., 2002, 2005, 2014; Lowe and Anderson, 2003; Graham et al., 2009; Larter et al., 2009, 2014; Jakobsson et al., 2012; Klages et al., 2015).

3. Data and methods

3.1. Multibeam bathymetric data

Seafloor morphology data were derived from shipborne multibeam-bathymetric surveys of four regions of the Antarctic continental shelf: the Anvers-Hugo Trough and Marguerite Bay in the western Antarctic Peninsula, and Pine Island Bay and a region offshore of the Dotson-Getz

Table 1
Details of the cruise datasets used in this investigation, separated into study regions.

Year	Cruise/ID	Ship	Multibeam system	Principal investigator
Anvers-Hugo Trough				
1991	EW9101	Maurice Ewing	Hydrosweep DS	Hayes, D.
1999	NBP9902	Nathaniel B. Palmer	SeaBeam 2112	Anderson, J.
1999	NBP9903	Nathaniel B. Palmer	SeaBeam 2112	Domack, E.
1999	NBP9905	Nathaniel B. Palmer	SeaBeam 2112	Wiens, D.
2000	NBP0001	Nathaniel B. Palmer	SeaBeam 2112	Jacobs, S.
2001	NBP0104	Nathaniel B. Palmer	SeaBeam 2112	Wiebe, P.
2001	NBP0107	Nathaniel B. Palmer	SeaBeam 2112	Domack, E.
2001	JR67-JR69	James Clark Ross	EM120	Bacon, S.
2002	NBP0201	Nathaniel B. Palmer	SeaBeam 2112	Anderson, J.
2002	NBP0202	Nathaniel B. Palmer	SeaBeam 2112	Wiebe, P.
2002	JR71	James Clark Ross	EM120	Pudsey, C. & Dowdeswell, J.
2002	JR81	James Clark Ross	EM120	Bacon, S.
2003	JR84	James Clark Ross	EM120	Jenkins, A. & Dowdeswell, J.
2005	–	HMS Endurance	EM710S	–
2005	NBP0502	Nathaniel B. Palmer	EM120	Anderson, J.
2005	JR112	James Clark Ross	EM120	Brandon, M.
2006	–	HMS Endurance	EM710S	–
2006	NBP0602	Nathaniel B. Palmer	EM120	Stock, J. & Cande, S.
2006	NBP0703	Nathaniel B. Palmer	EM120	Anderson, J. & Hallet, B.
2006	JR157-166	James Clark Ross	EM120	Dowdeswell, J.
2006	JR158	James Clark Ross	EM120	Luijtung, H.
2006	JR165	James Clark Ross	EM120	Shoosmith, D.
2007	JR179	James Clark Ross	EM120	Larter, R.
2007	JR185	James Clark Ross	EM120	Fielding, S.
2007	JR193-196	James Clark Ross	EM120	Quartly, G.
2008	–	HMS Endurance	EM710S	–
2008	JR188	James Clark Ross	EM120	Waluda, C.
2009	–	HMS Scott	SASS IV	–
2009	JR228	James Clark Ross	EM120	Watkins, J. L.
2010	JR240	James Clark Ross	EM120	Maksym, E.
2011	–	HMS Protector	EM710	–
2011	JR254D-264-265	James Clark Ross	EM120	Yelland, M. J. & Morales Maqueda, M. A.
2012	JR279-286	James Clark Ross	EM120	Morales Maqueda, M. A.
2014	JR284	James Clark Ross	EM122	Larter, R.
2015	–	HMS Protector	EM710	–
2016	–	HMS Protector	EM710	–
Marguerite Bay				
1991	EW9101	Maurice Ewing	Hydrosweep DS	Hayes, D.

Table 1 (*continued*)

Year	Cruise/ID	Ship	Multibeam system	Principal investigator
1999	NBP9902	Nathaniel B. Palmer	SeaBeam 2112	Anderson, J.
1999	NBP9903	Nathaniel B. Palmer	SeaBeam 2112	Domack, E.
2000	NBP0001	Nathaniel B. Palmer	SeaBeam 2112	Jacobs, S.
2001	NBP0103	Nathaniel B. Palmer	SeaBeam 2112	Wiebe, P.
2001	NBP0104	Nathaniel B. Palmer	SeaBeam 2112	Wiebe, P.
2001	JR59	James Clark Ross	EM120	Pudsey, C.
2001	JR67-69	James Clark Ross	EM120	Collins, J.
2002	NBP0201	Nathaniel B. Palmer	SeaBeam 2112	Anderson, J.
2002	NBP0202	Nathaniel B. Palmer	SeaBeam 2112	Wiebe, P.
2002	JR71	James Clark Ross	EM120	Pudsey, C. & Dowdeswell, J.
2003	JR84	James Clark Ross	EM120	Jenkins, A. & Dowdeswell, J.
2004	JR104	James Clark Ross	EM120	Larter, R.
2005	JR112	James Clark Ross	EM120	Brandon, M.
2004	JR115	James Clark Ross	EM120	Sparrow, M. D. & Hawker, E. J.
2007	JR157-166	James Clark Ross	EM120	Dowdeswell, J.
2007	JR158	James Clark Ross	EM120	Luijtung, H.
2007	JR165	James Clark Ross	EM120	Shoosmith, D.
2007	JR185	James Clark Ross	EM120	Fielding, S.
2007	NBP0702	Nathaniel B. Palmer	EM120	Nitsche, F.
2008	JR179	James Clark Ross	EM120	Larter, R.
2008	JR194-197	James Clark Ross	EM120	Quartly, G.
2009	JR188	James Clark Ross	EM120	Waluda, C.
2010	JR193-196	James Clark Ross	EM120	Quartly, G.
Pine Island Bay & Dotson-Getz ice shelves				
1999	NBP9902	Nathaniel B. Palmer	SeaBeam 2112	Anderson, J.
2000	NBP0001	Nathaniel B. Palmer	SeaBeam 2112	Jacobs, S.
2006	JR141	James Clark Ross	EM120	Larter, R.
2006	ANT-XXIII/4	Polarstern	Hydrosweep DS2	Gohl, K.
2007	NBP0702	Nathaniel B. Palmer	EM120	Nitsche, F.
2008	JR179	James Clark Ross	EM120	Larter, R.
2009	NBP0901	Nathaniel B. Palmer	EM120	Jacobs, S.
2010	ANT-XXVI/3	Polarstern	Hydrosweep DS2	Gohl, K.
2014	JR294	James Clark Ross	EM122	Heywood, K.

ice shelves in the Amundsen Sea Embayment (Fig. 1). These cruise data are summarised in Table 1. The data were collected over the last two decades using a variety of multibeam systems including Kongsberg EM120/EM122 multibeam echo sounders with a transmission frequency of 11.25–12.75 kHz and a swath angle of up to 150° (for data collected by the RRS *James Clark Ross* and, post-2002, the RVIB *Nathaniel B. Palmer*); Krupp-Atlas Hydrosweep DS multibeam echo sounders with a transmission frequency of ~15 kHz and a swath angle of up to 120° (for data collected by the RV *Maurice Ewing* and RV *Polarstern*); and Seabeam 2112 multibeam sonar systems with a transmission frequency of 12 kHz and

a swath angle of up to 120° (for data collected by the RVIB *Nathaniel B. Palmer* until 2002) (Nitsche et al., 2007 and references therein). The vertical resolution of multibeam echo sounder data is typically a few metres, whilst horizontal resolution varies according to the grid size specified when processing the bathymetric data (Wellner et al., 2006; Jakobsson et al., 2016); this is usually between 5 and 50 m.

The bathymetric data were processed and gridded into a digital elevation model (DEM) using open access MB-System software (Caress and Chayes, 2004; Caress et al., 2020). A conservative degree of interpolation, applied up to four cell widths away from a data-filled cell, was used to fill small missing gaps in the grids when proximal to existing multibeam bathymetry data. Obtaining detailed, yet accurate, channel cross-sectional profiles requires a trade-off between a high-resolution grid size and over-reliance on interpolation, which may introduce errors into the sampled cross-sectional geometries. Initial sensitivity experiments with horizontal grid spacing between 10 and 100 m revealed that the grid resolution had a significant effect on the channel morphology, as grid resolutions coarser than 30 m altered the maximum depth and curvature of the channel. In order to preserve geomorphic detail within the sampled channel cross sections, the multibeam bathymetry data were gridded at the highest resolution that could be achieved without requiring interpolation to fill >10% of the study area's grid cells. Application of this technique permitted data from the Anvers-Hugo Trough, Marguerite Bay and Pine Island Bay to be gridded at a 20-m resolution, whilst the area offshore of the Dotson-Getz ice shelves was gridded at a 30-m resolution.

3.2. Channel delineation and channel metric derivation

The channel-mapping inventory was completed in ArcGIS 10.4 using hill-shaded DEMs. Mapping accuracy was verified by draping the digitised channel outlines over a three-dimensional representation of the DEM (Mayer et al., 2000). In this manner, the routing pathway of each individual channel was established. Channels were defined to terminate when they were intersected by a larger, deeper routing pathway or once they entered a basin. Once the channel inventory was complete, cross sections were extracted perpendicular to the long axis of each individual channel using a ~1 km sampling interval to ensure that even relatively short channels were sampled multiple times. Approximately 10,000 channel cross sections were extracted across the four study sites on the west Antarctic continental shelf. Each cross-sectional profile was visualised and manually verified to prevent the inclusion of erroneous channel mappings in the inventory.

The width, depth, cross-sectional area, symmetry, and shape of each channel cross section were quantified using a semi-automated algorithm (Noormets et al., 2009; Kirkham et al., 2019). Width is defined as the distance between the highest point of each of the channel sides. The greatest vertical distance between the base of the channel and a line intersecting the two channel edges defines the channel depth, *D*. The horizontal distances from the deepest point of the channel to each of the channel sides, *W1* and *W2*, are calculated using an idealised triangular representation of the channel. The normalised ratio of *W1* to *W2* is used to assess the symmetry of the channel, *A*, which can range between 0 and 2, with $A = 1$ indicating a symmetrical cross-section, $A > 1$ signifying a left-skewed channel (channel with a longer left-hand side) and $A < 1$ indicating a right-skewed channel cross-section. Trapezoidal numerical integration was used to approximate the internal area of the channel, bounded by the line intersecting the channel edges. The ratio of channel depth to channel width, or form ratio (Graf, 1970), was used to enable comparison between the vertical and horizontal proportions of each cross section:

$$\text{form ratio} = \frac{D}{(W1 + W2)} \tag{1}$$

In addition to the form ratio, the cross-sectional shape of each channel was assessed using the General Power Law (GPL) program of Pattyn and Van Huele (1998). The GPL program applies a general form of the power-law equation to derive a best-fit approximation of a shape parameter, *b*, which summarises the geometric shape of the channel:

$$y - y_0 = a|\, x - x_0 \,|^b \tag{2}$$

where *a* and *b* are constants, x_0 and y_0 are the coordinates of the origin of the cross profile and *x* and *y* are the horizontal and vertical components of the channel cross section, respectively. A general least-squares method is used to derive the best-fit values of *a* and *b*. The value of the shape parameter, *b*, generally varies from 1 to 2 according to cross-sectional shape. A *b*-value of 1 indicates a perfectly 'V-shaped' channel cross-section, whilst a value of 2 denotes a perfect 'U'-shape (Pattyn and Van Huele, 1998). Values between 1 and 2 indicate a combination of V- and U-shaped channel geometries. Shape parameter values exceeding 2 are associated with more box-shaped channel cross-sectional profiles, whilst geometries characterised by a *b*-value <1 indicate a convex-upward channel form (Gales et al., 2013). The sinuosity of the longitudinal profile of each individual channel was also calculated by dividing the overall length of each channel by the straight-line distance between its two vertices. A sinuosity index of 1 denotes a perfectly straight channel, whilst values >1.05 are associated with sinuous channel forms (Mangold et al., 2010). The compass angle of a straight line intersecting both end nodes of a profile defines the channel orientation.

3.3. Comparison of channel metrics

Moment-ratio plots (Craig, 1936; Johnson and Kotz, 1970) were used to determine with a statistical basis the distributional form taken by the channel metrics for each study site. Moment-ratio plots summarise an empirical distribution as a single point derived from a pair of standardised moments (Vargo et al., 2010). The plot visualises specific distributions as points or curves, whilst generalised distributional families such as Paretos, lognormals and exponentials are represented as discrete areas (Cirillo, 2013). Moment-ratio plots also contain a 'grey zone' composed of a range of power-law tails and lognormal distributions. The zone within which a point falls relates to the underlying distributional form of the empirical data (Vargo et al., 2010). For the method employed here, standardised moments refer to the coefficient of variation, *CV*, and skewness, γ_3, defined as:

$$CV = \frac{\sigma_X}{\mu_X} \tag{3}$$

$$\gamma_3 = K\left[\left(\frac{X - \mu_X}{\sigma_X}\right)^3\right] \tag{4}$$

where μ_X and σ_X are the mean and standard deviation of the variable *X*, respectively. K is the expectation operator.

In addition to the moment-ratio analysis, principal components analysis (PCA) was employed to examine whether the four study areas could be distinguished from one another based on their calculated channel metrics. PCA is a multivariate statistical technique used to examine subtle trends in datasets containing multiple variables. PCA effectively reduces the dimensionality of datasets by transforming multiple variables into linearly related combinations that explain the maximum amount of variance present in the data (Jolliffe, 2002). PCA therefore identifies directions, termed principal components, along which data variance is maximal (Pope and Rees, 2014). The first principal component (PC1) is defined as the linear combination of the variables that account for the greatest proportion of total variation in the data. The second principal component (PC2) is the direction with the next highest variance that is uncorrelated to the first principal component (Ringnér, 2008), and so forth. As the channel metrics vary over different scales

and are of different units, the parameters were first normalised to convert them to dimensionless units before a correlation matrix was calculated. PCA was then conducted and, following Mandal et al. (2008), eigenvalues under 1 were excluded from the analysis. Component scores for all the components with eigenvalues >1 were plotted to demonstrate which variables explained the greatest degree of variance in the data.

4. Results

4.1. Description of mapped channels

4.1.1. Anvers-Hugo Trough

The Anvers-Hugo Trough is a glacially eroded trough situated offshore of Graham Land, western Antarctic Peninsula (Fig. 1). Multibeam-bathymetric coverage of this region contains a large, ~1400-m-deep, seafloor depression termed the Palmer Deep Basin (Domack et al., 2006) which is situated directly to the south of Anvers Island. Data coverage then extends westwards from the Palmer Deep Basin across the Palmer Deep Outlet Sill and into the Anvers-Hugo Trough, which trends northwards towards the continental shelf edge (Larter et al., 2019). Approximately 600 bedrock channels were mapped from the seafloor DEM, occupying an area of ~16,500 km^2 (Figs. 2a, 3a). The majority of the observed channels are <5000 m long; this reflects the dendritic nature of channel connections within the Anvers-Hugo Trough where smaller channels are captured by larger ones, although the degree to which a lack of spatial coverage limits the true length of the surveyed channels is uncertain. The channels are predominantly sinuous, with most sinuosity indexes >1.05. Where present, straighter channels are typically shorter than 5000 m in length. Longitudinal channel profiles display meandering thalwegs with reverse-slope gradients along sections of the channel long profiles (Fig. 4a).

Channel cross-sectional analysis reveals that the channels are 80–1700 m wide (mean = 330 m), 3–240 m deep (mean = 37 m), and exhibit cross-sectional areas of 160–160,000 m^2 (mean = 9400 m^2) (Table 2). The largest channels connect to the Palmer Deep Basin from both the west over the Palmer Deep Outlet Sill and from the northeast, south of Anvers Island. Channel form ratios range between 0.02 and 0.48 (mean = 0.14), with channels being on average seven times as wide as they are deep. Channel *b*-values are characterised by an interquartile range of 1.1–1.6, with the average *b*-value of 1.3 denoting that most channels possess V-shaped cross sections. The channel cross sections exhibit a broad range of symmetry values (from 0 to 2), indicating that there is no preferential symmetrical orientation for each channel; no spatial clustering of symmetry values is present.

4.1.2. Marguerite Bay

Channelised landforms within Marguerite Bay are situated on the inner-shelf portion of Marguerite Trough. This trough housed the largest palaeo-ice stream that drained the Pacific side of the Antarctic Peninsula Ice Sheet (Livingstone et al., 2012; Hernández-Molina et al., 2017) (Fig. 1). The >250-km-long trough runs obliquely across the continental shelf in an approximately north-south direction, bounded by Adelaide Island to the northeast and Alexander Island to the southwest (Figs. 2b, 3b). The trough is ~50 km across and reaches depths of over 1600 m on the inner shelf before grading into a wider (>70 km), shallower feature on the outer shelf with only 50–70 m of relief in water depths of 400–500 m.

The 1055 channels present within the ~35,000 km^2 inner-shelf region are incised into bedrock and orientated predominantly northwards along the long axis of the trough, and southwest in the region southeast of Adelaide Island. No channels are observed on the outer continental shelf beyond the transition between the inner-shelf bedrock substrate and the outer shelf sedimentary strata (Fig. 2b; Anderson and Oakes-Fretwell, 2008). The channels possess meandering thalwegs and contain sections with reverse-slope gradients (Fig. 4b). They are arranged in a relatively dendritic pattern, with smaller channels coalescing to feed wider and deeper channels in the trough's central portion downstream. The majority of channels within Marguerite Trough are relatively straight and short (<5000 m long), although the longest channels, which flow parallel to the long axis of the basin, may exceed 50 km in length. Southeast of Adelaide Island, the channels exhibit a more anastomosing pattern comprising of sinuous channels <5000 m long.

The channels range in width between 80 m and 2900 m (mean = 400 m), span depths of 3 m to 200 m (mean = 40 m) and exhibit cross-sectional areas of 160 m^2 to 276,000 m^2 (mean = 12,500 m^2). Channel form ratios range between 0.01 and 0.55, with the mean form ratio of 0.13 indicating that the channels are eight times as wide as they are deep on average. The range of channel form ratios decreases with increasing channel cross-sectional area, and tends towards a value of ~0.1 as the channels enlarge, suggesting that the width of the channel, rather than its depth, is the dominant control on its shape. Channels generally exhibit asymmetrical cross-sectional geometries, yet there are no spatial trends in channel symmetry across the trough. The interquartile range of cross-sectional *b*-values falls between 1.0 and 1.5, with an average of 1.2 indicating predominantly V-shaped cross-sectional geometries.

4.1.3. Pine Island Bay

Multibeam-bathymetric coverage of Pine Island Bay includes most of the inner shelf portion of Pine Island Trough — a channelised ~19,000 km^2 region of the inner continental shelf that extends >400 km northwards from the terminus of the Pine Island Ice Shelf towards the continental-shelf break (Figs. 2c, 3c). Channels are present across almost all of the inner continental shelf region covered by existing bathymetric datasets. No channels exist beyond the transition from the inner-shelf bedrock to the middle- and outer-shelf sedimentary strata (Lowe and Anderson, 2002; Gohl et al., 2013). Over 1000 channels are identified in Pine Island Bay. The interconnected channels are arranged in a complex anastomosing pattern with no predominant orientation, instead appearing to follow lines of geological weakness in the inner-shelf bedrock. Channel longitudinal profiles exhibit meandering thalwegs with intermittent reverse-slope gradients (Fig. 4c). The majority of channels are <5000 m long and have sinuosity indexes >1.05.

The channels are 80–3600 m wide (mean = 507 m), 3–330 m deep (mean = 43 m), and exhibit cross-sectional areas of 590–290,000 m^2 (mean = 17,000 m^2). Channel form ratios range between 0.01 and 0.44, with the average channel being approximately ten times as wide as it is deep. Form ratio generally decreases with increasing cross-sectional area, denoting that width is the dominant control on channel shape, and that larger channels are disproportionally wide relative to their depth. The majority of channel cross sections are asymmetric, although no preferential direction of skewness is favoured. The *b*-values of the channels exhibit lower and upper quartiles of 0.9 and 1.4, respectively, with an average *b*-value of 1.1 denoting that the channels are predominantly V-shaped.

4.1.4. Dotson-Getz area

Multibeam-bathymetric data coverage in the region offshore of the Dotson and Getz ice shelves extends ~100 km offshore of the contemporary ice margin, spanning an area of ~30,000 km^2 (Fig. 1). The regional bathymetry of the area consists of three glacial troughs situated offshore of their respective modern ice shelves that converge northwards into the main Dotson-Getz cross-shelf trough which continues towards the continental-shelf break (Fig. 2d). Over 350 channels incise the inner-shelf bedrock, covering an area of 16,000 km^2. Channels occur most densely within the Getz B cross-shelf trough. No channels are present on the outer shelf where there are thick sedimentary strata and soft sediments occur at the seafloor (Gohl et al., 2013). The channels are predominantly orientated parallel to the long axis of the troughs and, in the case of Getz B, tend towards an increasingly dendritic pattern with

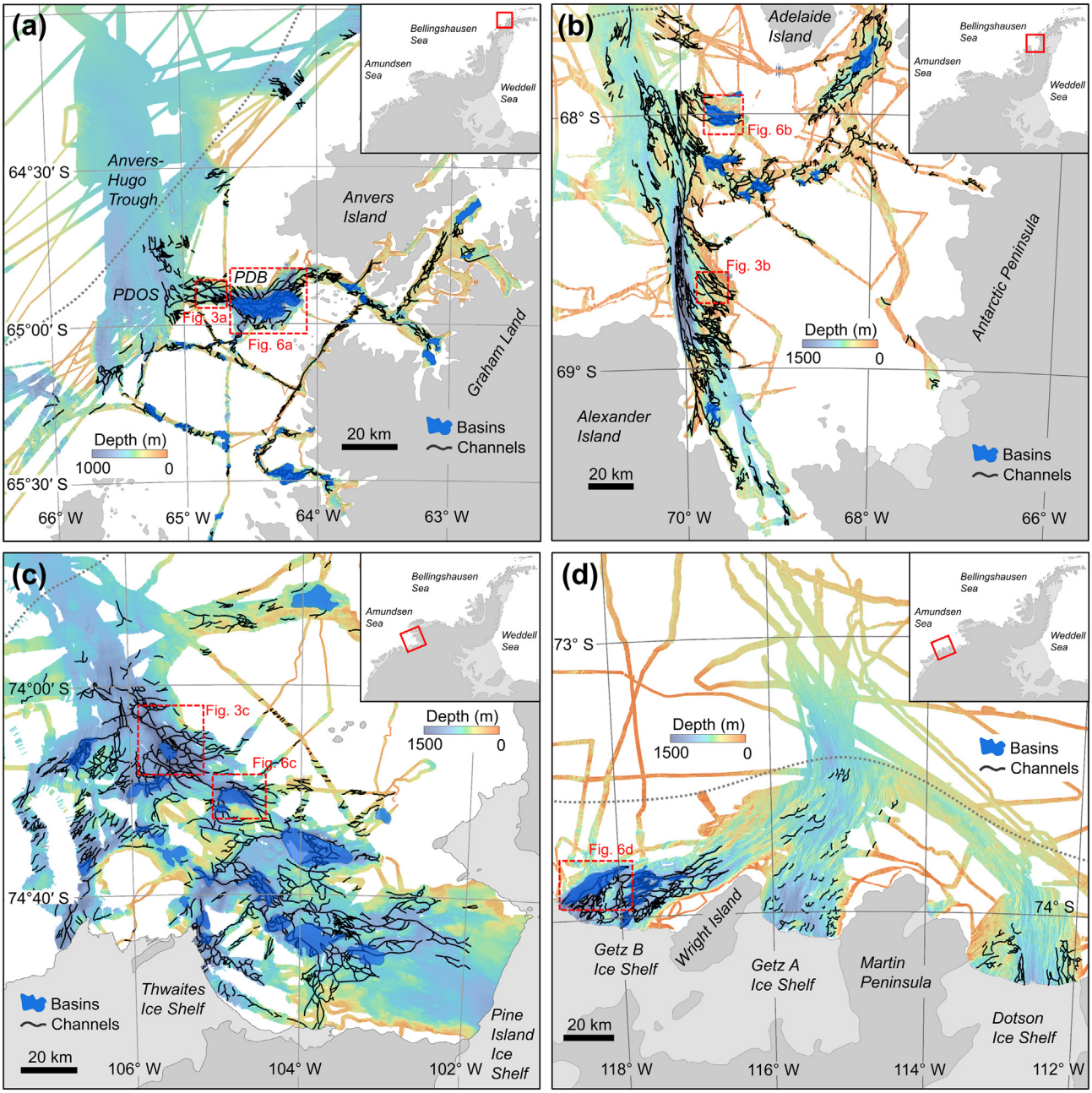

Fig. 2. Bedrock channels on Antarctic inner continental shelves. Detailed multibeam bathymetry of: (a) Anvers-Hugo Trough, (b) Marguerite Bay, (c) Pine Island Bay, and (d) offshore of the Dotson-Getz ice shelves with channels displayed as black lines and basins shown as blue polygons. The boundary between inner-shelf bedrock and outer shelf sedimentary strata is displayed as a dotted grey line. The abbreviations PDB and PDOS in (a) refer to the Palmer Deep Basin and Palmer Deep Outlet Sill, respectively. The locations of the channels displayed in Fig. 3 and the basins displayed in Fig. 6 are shown.

distance away from the current ice-sheet margin. The majority of the channels are <5000 m long and cluster along the edges of the troughs. Longer channels are less common, but some do occur in the centre of the troughs. Owing to the higher density of channels present offshore of the Getz B Ice Shelf compared to the other troughs, the dominant channel orientation over the whole Dotson-Getz shelf is northeast which primarily reflects the orientation of the long axis of the Getz B trough. The majority of channels are sinuous, and any straight channels tend to be <5000 m in length. All channels possess meandering thalwegs that have sections with reverse-slope gradients (Fig. 4d).

Channel cross sections range in width between 75 m and 2400 m (mean = 570 m), vary in depth between 4 m and 280 m (mean = 50 m), and exhibit cross-sectional areas between 170 m^2 and 207,000 m^2 (mean = 22,000 m^2). Channel form ratios range between 0.02 and 0.42, with the average channel nine times as wide as it is deep. Form ratios tend towards a value of 0.15 with increasing cross-sectional area, implying that channel width is the dominant control on channel shape, with width increasing non-linearly with depth. Channel cross sections are typically asymmetric, and no overall tendency towards right or left skewness is present. A *b*-value interquartile range of 0.9–1.4 and an average *b*-value of 1.1 suggests that the channels are predominantly V-shaped.

4.2. Regional comparison of channel morphometry

The channels mapped across the four continental shelf areas are characterised by remarkably similar morphometric properties. The

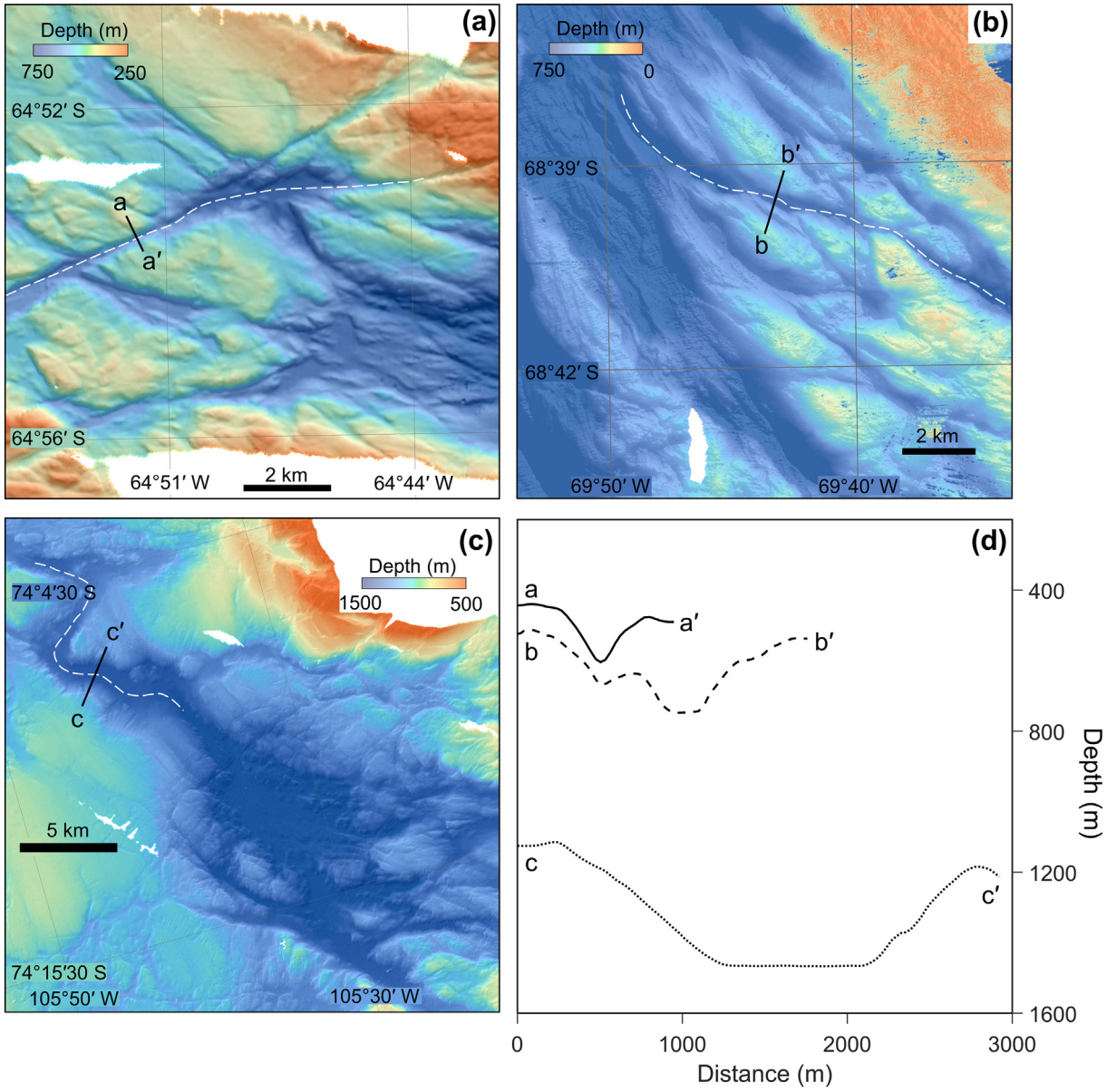

Fig. 3. Bedrock channels incised into Antarctic inner continental shelves. Examples of channels present in: (a) Anvers-Hugo Trough, (b) Marguerite Bay, and (c) Pine Island Bay. Panel (d) displays cross sections of some of the example channels, with their locations marked as a solid black line in their respective figure panels. Vertical exaggeration in (d) is ~2×. White dashed lines in (a–c) indicate the locations of the longitudinal profiles displayed in Fig. 4.

widths, depths and cross-sectional areas of the channels exhibit similar minimum, maximum, and mean values (Table 2). These parameters are lognormally distributed as a result of larger numbers of comparatively smaller channels versus smaller numbers of larger ones (Fig. 5). Channels in all four regions are 2–50+ times wider than they are deep, with an average form ratio of ~0.13 indicating that most channels are approximately seven to eight times as wide as they are deep. For all four regions, lower channel form ratios are associated with greater channel widths and cross-sectional areas. Although a weak positive correlation is present between increasing form ratio and increasing depth ($r = 0.37$ to 0.48), channel width is the dominant control on channel shape. Based on decreasing variances of form ratio with increasing channel cross-sectional area, it appears that the cross-sectional geometries of channels in all regions tend towards a consistent profile shape as they enlarge. The variation of *b*-values with channel size supports this interpretation, as channels tend towards a *b*-value of ~1.1 as the dimensions of the channels increase. The cross-sectional profiles of the channels are typically asymmetric, although no direction of asymmetry is favoured (Fig. 5). Whilst channel morphometries are highly similar between the four continental shelf regions, the channels in the Amundsen Sea are slightly larger on average than those in the western Antarctic Peninsula. This difference stems from the channels in the Amundsen Sea being comparatively wider and deeper on average (560–570 m and 50 m, respectively) than those observed in the western Antarctic Peninsula (330–400 m and 37–40 m, respectively).

4.3. Description of mapped basins

In addition to the channels, 59 bedrock basins are mapped in the multibeam coverage of the seafloor of the western Antarctic Peninsula and Amundsen Sea regions (Fig. 6). The basins are flat-bottomed depressions with relatively steep (20–40°) bounding slopes. They are distinct from the channels due to their larger dimensions and their wholly different morphologies including non-parallel sides, lower length-

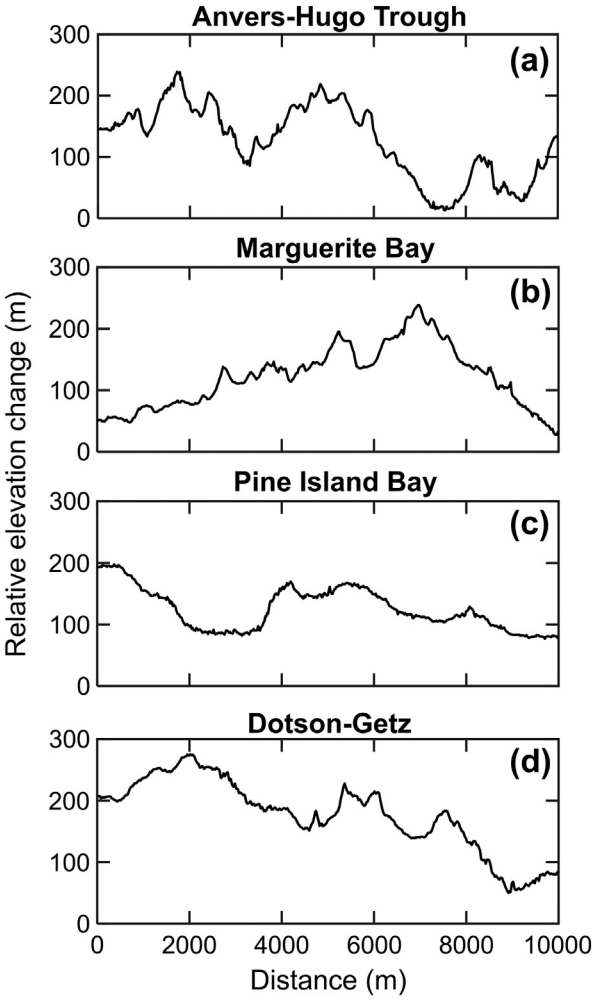

Fig. 4. Typical longitudinal channel profiles. Channels in all study regions possess thalwegs with reverse-sloping gradients and similar along-profile changes in relative elevation. Profiles are taken from offshore (left side of figure) to inshore (right side of figure). The locations of profiles (a), (b), and (c) are displayed in Fig. 3. Profile (d) is from the Getz B trough. Vertical exaggeration is 13×.

width ratios, irregular shapes and flat bottoms (Figs. 3 and 5). The majority of the basins are <10,000 m long, <5000 m wide and <10 km^2 in planimetric area. The basins are typically 2.1 times as long as they are wide ($r = 0.90$, $p < 0.01$) (Fig. 7). All of the basins are connected by channel networks and many contain subdued linear or drumlin-shaped features that are overlain by a thin (<5 m thick) veneer of post-glacial fine-grained sediment (e.g. Nitsche et al., 2013).

Basins occur most frequently in the region of Anvers-Hugo Trough, which exhibits 27 bedrock depressions ranging in planimetric area from 0.13 km^2 to the 150 km^2 Palmer Deep Basin, which dominates the bathymetry of this area (Fig. 2a). A further nine basins, morphologically similar to those in the Anvers-Hugo Trough, are observed in Marguerite Bay (Fig. 2b). The majority of basins in Marguerite Bay are clustered in a region ~40 km south of Adelaide Island, and range in planimetric areal extent between 6 km^2 and 88 km^2. Like the Anvers-Hugo Trough, the bedrock basins in Marguerite Bay are connected by a series of channels that feed into the basins and frequently incise into the base of the depressions. In the Amundsen Sea, 19 flat-bottomed depressions with planimetric areas of 5–160 km^2 were mapped in Pine Island Bay (Fig. 2c), whilst a further four basins are present within the Getz B trough, ranging in planimetric area between 11 km^2 and 276 km^2 (Fig. 2d).

4.4. Principal components analysis

Principal components analysis was employed to further examine whether the four study areas could be distinguished from one another on the basis of their channel metrics. PC1 and PC2 had eigenvalues >1, and were assumed to best represent the variance in the data; they were therefore retained for further analysis. PC1 represents 41% of the total variance, whilst PC2 represents 24% of variance, with most of the variability in PC1 relating to cross-sectional area (eigenvector = 0.616), and the dominant variability in PC2 being due to form ratio (eigenvector = 0.763) (Table 3). The pattern displayed in Fig. 8 demonstrates tight clustering of the first and second principal components for all four study regions, implying that all sites exhibit similar morphological characteristics.

5. Interpretation and discussion

5.1. Interpretation of the channels

The channels incised into bedrock on the inner continental shelves of the Amundsen Sea and the western Antarctic Peninsula occur within large glacially-eroded troughs that extend across the Antarctic continental shelf. Diagnostic subglacial bedforms, including mega-scale glacial lineations (Clark, 1993), which have been observed to form under modern ice streams (King et al., 2009), indicate that these cross-shelf troughs were occupied by fast-flowing ice during former glacial periods (Stokes and Clark, 2002; Ottesen et al., 2005, 2007; Larter et al., 2009; Dowdeswell et al., 2010; Graham et al., 2010; Livingstone et al., 2012). The presence of bifurcating and anastomosing channel systems containing abandoned loops, abrupt terminations and initiations, combined with their undulating thalwegs, is characteristic of erosion by pressurised subglacial meltwater flowing under ice (Shreve, 1972; Sugden et al., 1991; Lowe and Anderson, 2003; Lewis et al., 2006; Greenwood et al., 2007; Nitsche et al., 2013; Domack et al., 2016; Galofre et al., 2018). The similar geometries, scaling characteristics, and spatial structures of the channels present within the inner, largely bedrock-floored, regions of the different Antarctic cross-shelf troughs imply that the features were produced by the same mechanism: incision by subglacial meltwater flowing beneath the formerly expanded outlets of the Antarctic Ice Sheet.

The interpretation that the channel systems present in the Anvers-Hugo Trough, Marguerite Bay, Pine Island Bay, and just seaward of the Dotson-Getz ice shelves are the product of pressurised subglacial meltwater is supported by high-resolution, remotely operated underwater

Table 2
Extracted channel parameters for the four study regions. The minimum, maximum and mean of the extracted parameter distributions are used as descriptors for each metric. For the *b*-value parameter, L.Q. and U.Q. refer to the lower and upper quartiles of the distribution, respectively. The results of the symmetry parameter are not shown here due to consistently ranging between 0 and 2, and often exhibiting a double-peaked distributional geometry, which would render the use of the mean as a statistical descriptor misleading.

Study region	Width (m)			Depth (m)			Area (m^2)			Form ratio			*b*-value		
	Min.	Max.	Mean	Min.	Max.	Mean	Min.	Max.	Mean	Min.	Max.	Mean	L.Q.	U.Q.	Mean
Anvers-Hugo Trough	80	1700	330	3	240	37	160	160,000	9400	0.02	0.48	0.14	1.1	1.6	1.3
Marguerite Bay	80	2900	400	2.6	200	40	160	276,000	12,500	0.01	0.55	0.13	1.0	1.5	1.2
Pine Island Bay	80	3400	560	3	216	50	590	290,000	20,000	0.01	0.44	0.13	0.9	1.4	1.1
Dotson-Getz	75	2400	570	4	280	50	170	207,000	22,000	0.02	0.42	0.11	0.9	1.4	1.1

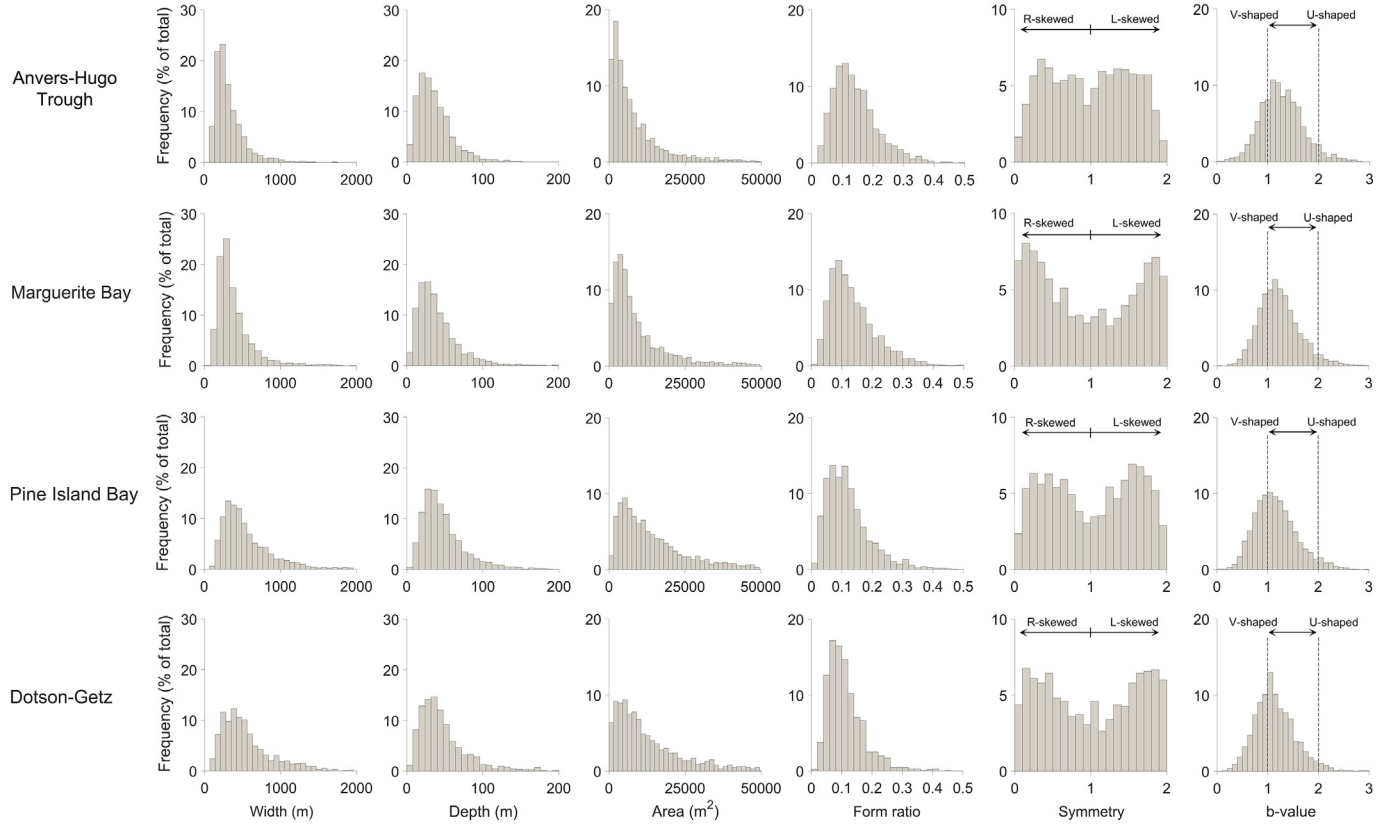

Fig. 5. Size-frequency distributions of the six channel metric parameters for each study region. The dotted lines in the *b*-value plots correspond to where idealised V-shaped ($b = 1$) and U-shaped ($b = 2$) cross sections would fall on the histogram.

vehicle imagery from Marguerite Bay. This imagery reveals that the channels have steep sidewalls and contain potholes eroded into bedrock (Hogan et al., 2016). Flow velocities >10 m s^{-1}, together with a suitable bedload to act as an erosive agent, are required for pothole formation (Sugden et al., 1991), implying that the channels are the product of fast-flowing water. Furthermore, their typical form ratios and *b*-values indicate that the channels exhibit broad and shallow V-shaped cross-sectional profiles, instead of the U-shaped morphologies associated with direct glacial erosion (Harbor, 1992). A V-shaped morphology is indicative of subglacial meltwater erosion (Rose et al., 2014), which incises down into the channel floor rather than widening the sidewalls (van Dijke and Veldkamp, 1996).

The generally oblique channel orientation with reference to the along-trough ice-flow direction, as interpreted from the orientation of subglacial bedforms in all study regions (Domack et al., 2006; Ó Cofaigh et al., 2008; Larter et al., 2009), combined with their overdeepened thalwegs, suggests that the channels were not formed directly by the action of grounded ice (Nitsche et al., 2013). Rather, the extensive areas over which the meltwater channels are observed indicate that, when active, the subglacial hydrological system of the ice formerly occupying these regions contained abundant subglacial meltwater that was consistently focussed along the same routing pathways by the subglacial water pressure gradient imposed by the overall ice-surface slope (Shreve, 1972, 1985; Dowdeswell et al., 2016). The tendency to observe greater quantities of smaller, anastomosing channels along the flanks of the inner cross-shelf troughs in Marguerite Bay, Pine Island Bay and offshore of the Dotson-Getz ice shelves may reflect the generation of greater quantities of meltwater through strain heating at the palaeo-ice stream shear margins (Graham et al., 2009; Perol et al., 2015; Meyer et al., 2016; Bougamont et al., 2019). Basal hydraulic gradients resulting from thicker ice in the centre of the troughs would drive the generated meltwater towards the ice-stream margin (Noormets et al., 2009; Dowdeswell et al., 2015), explaining the tendency for the meltwater channels to converge into fewer, straighter networks in the central portion of the troughs as they extend towards the continental shelf break (Lowe and Anderson, 2002). At a local scale, pre-existing structural weaknesses in bedrock geology would have acted as an additional control on the locations of meltwater channel erosion and flow routing (Lowe and Anderson, 2003).

5.2. Channel formation

Numerical modelling of subglacial water flow beneath Pine Island and Thwaites glaciers during the Last Glacial Maximum demonstrates that the bedrock channels in Pine Island Bay would have been capable of accommodating discharges of up to 8.8×10^6 m^3 s^{-1} if filled to the bankfull level (Kirkham et al., 2019). Although this represents a maximum carrying capacity for the channels, it is several orders of magnitude larger than what would be generated by present day basal meltwater production rates beneath Pine Island and Thwaites glaciers (typically <5 m^3 s^{-1}; Bougamont et al., 2019), or those predicted under their expanded Last Glacial Maximum configuration (typically <20 m^3 s^{-1}; Kirkham et al., 2019). Accordingly, the steady state flow of water produced by basal melting alone would not have been capable of mobilising the bedload needed to erode such large channels (Alley et al., 1997; Lowe and Anderson, 2003; Cook et al., 2013; Nitsche et al., 2013). The mechanism responsible for channel formation was therefore likely episodic.

Although many mechanisms could be responsible for the formation of the channels, including propagation of surface meltwater to the bed of the ice sheet (Carlson et al., 2008; Jansen et al., 2014; Rose et al., 2014), similar to that observed on the margins of the

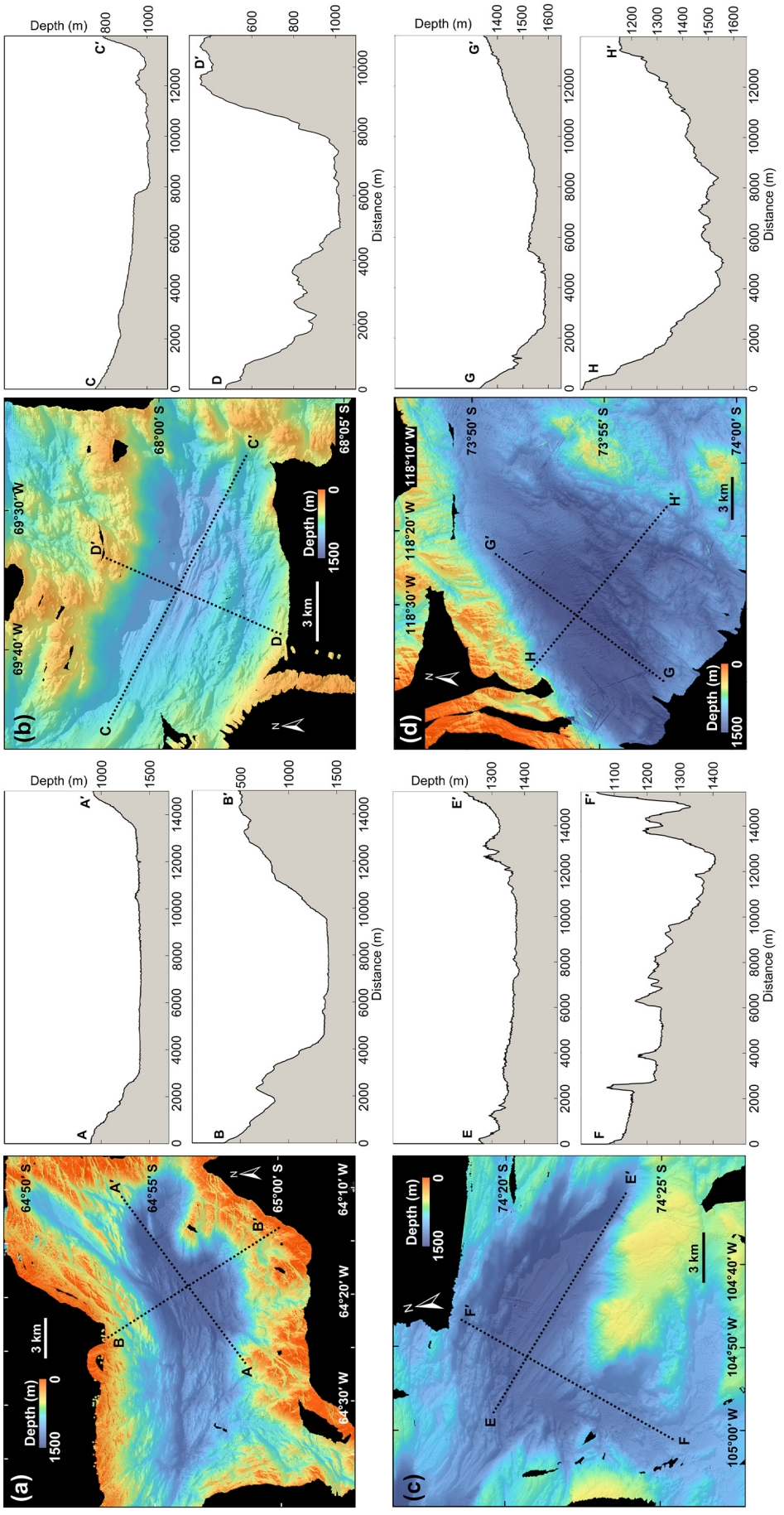

Fig. 6. Examples and cross-sectional profiles of bedrock basins in: (a) Anvers-Hugo Trough (the Palmer Deep Basin), (b) Marguerite Bay, (c) Pine Island Bay and (d) offshore of the Getz B Ice Shelf. The vertical exaggeration of cross-sectional profiles is 4× in (a), 10× in (b), 20× in (c) and 10× in (d).

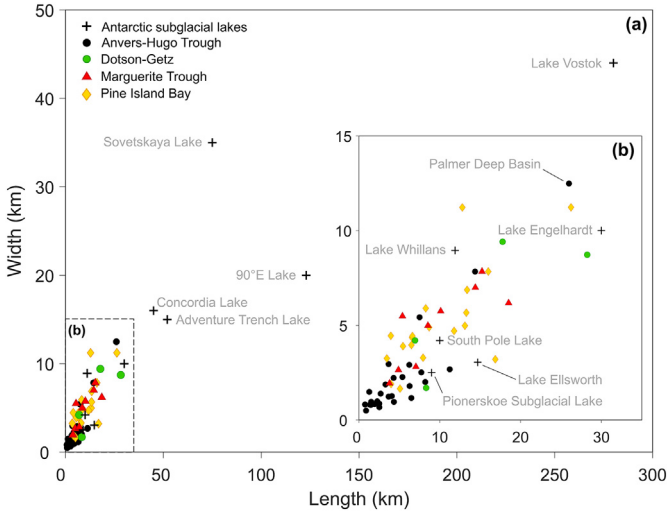

Fig. 7. Dimensions of bedrock basins. (a) Lengths and widths of the bedrock basins present within four offshore study sites compared to 10 Antarctic subglacial lakes with known dimensions (from Wright and Siegert, 2012). Inset figure (b) displays an enlarged version of (a), showing the 59 mapped offshore basins and 5 known subglacial lakes.

Table 3
Eigenvectors for the first and second principal components after variable normalisation.

Eigenvector	PC1	PC2
Width	0.561	−0.303
Depth	0.538	0.400
Area	0.616	0.019
Form ratio	−0.008	0.763
Symmetry	−0.001	0.032
b-value	−0.126	0.405

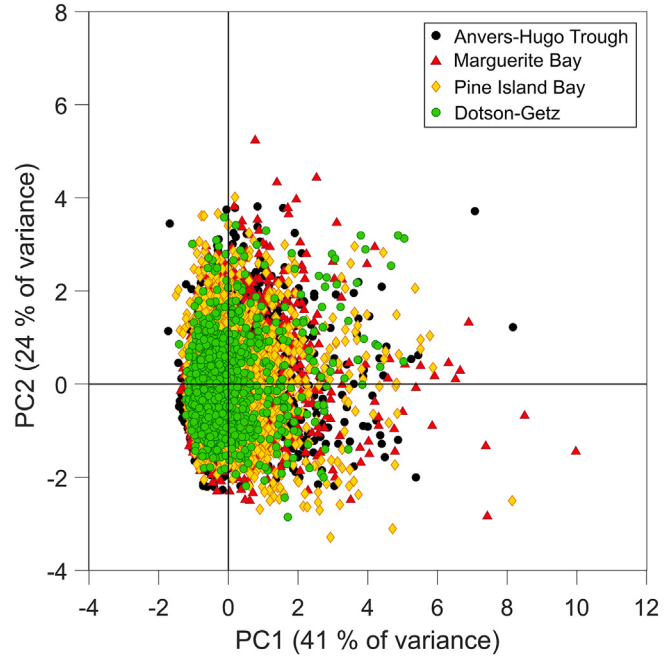

Fig. 8. Principal components analysis of channel width, depth, area, form ratio, sinuosity and *b*-value for the four study regions. Tight clustering between principal component 1 (PC1) and principal component 2 (PC2) is observed. Most variability in PC1 relates to cross-sectional area and the dominant variability in PC2 is due to form ratio.

contemporary Greenland Ice Sheet (Zwally et al., 2002; Das et al., 2008; Bartholomew et al., 2012; Cowton et al., 2012), or outburst floods triggered by subglacial volcanic eruptions (Nye, 1976; Björnsson, 2002; Roberts, 2005), the most likely mechanism is the drainage of subglacial lakes trapped in bedrock basins (Alley et al., 2006; Lewis et al., 2006; Jordan et al., 2010; Kirkham et al., 2019). Numerical calculations relating to this mechanism demonstrate that the cascading release of water trapped in a large upstream basin could initiate a flood with a peak discharge of up to ~5×10^5 m^3 s^{-1}, approximately the carrying capacity of the channels if they were partially ice filled at the time of the flood (Evatt et al., 2006; Kirkham et al., 2019). Lower-magnitude discharges from the drainage of individual lakes would also have had a significant erosive effect when repeated periodically over the duration of several glacial cycles (Beaud et al., 2018).

Inference of a subglacial lake drainage origin for the channels is also supported by an association between channel size and proximity to predicted subglacial lakes. For example, in Pine Island Bay, the largest bedrock channels are situated near to former lake basins, whilst smaller channels are located more distally (Kirkham et al., 2019). The bedrock channels incised into the continental shelf are also morphologically similar to channel systems that have been attributed to subglacial lake drainage elsewhere in Antarctica (Lewis et al., 2006). Furthermore, some channels possess trapezoidal cross-sectional shapes characterised by *b*-values of ~1.3–1.6 (Fig. 5). This cross-sectional shape has been associated with high-magnitude discharges of water released during outburst flooding in other settings (e.g. Bretz, 1923; Gupta et al., 2007; Larsen and Lamb, 2016).

Subglacial lake formation is favoured beneath ice streams because of enhanced meltwater production at the onset zones of streaming ice flow combined with very low hydraulic gradients (Bindschadler and Choi, 2007; Carter et al., 2007). This is demonstrated by the spatial distribution of subglacial lakes observed beneath the contemporary Antarctic Ice Sheet, where subglacial lakes tend to cluster in areas: i) proximal to ice divides where the ice surface slope and flow velocities are small; ii) at ice-stream onsets where frictional strain heating is prominent; and iii) in prominent subglacial troughs where ice is relatively thick (Siegert and Bamber, 2000; Siegert et al., 2005, 2016; Le Brocq et al., 2009). The largest subglacial lakes, such as the 14,000 km^2 Lake Vostok, appear to be tectonically controlled (Kapitsa et al., 1996; Dowdeswell and Siegert, 1999, 2003), whilst smaller lakes occur in glacially-scoured basins (Bell, 2008), similar in form to those exposed on the modern seafloor of the inner continental shelves of the Amundsen Sea and western Antarctic Peninsula. A third category of lakes consists of those which have been observed to periodically drain. Whilst there are some exceptions (Lake Whillans and three lakes in the Adventure Subglacial Trench), these lakes do not have the characteristic radar reflectance properties of bodies of deep water (>10 m) occupying distinct basins beneath the ice sheet (Wright and Siegert, 2012; Siegert et al., 2014), but can instead be identified through the localised rising and falling of the ice-sheet surface measured by satellite altimetry (e.g. Wingham et al., 2006; Fricker et al., 2007; Smith et al., 2009a). This class of lake is typically observed in regions of relatively high ice surface slope, which is unfavourable for long-term water ponding (Wright and Siegert, 2012). Consequently, these lakes likely represent shallow, ephemeral features of the subglacial hydrological system which store water for only a short time before transferring it elsewhere (Wright and Siegert, 2012; Siegert et al., 2014).

The 59 elongate, steep-sided overdeepened basins observed in the Anvers-Hugo Trough, Marguerite Bay, Pine Island Bay, and offshore of the Dotson-Getz ice shelves make them prime candidates for areas where subglacial water would be likely to pond, producing subglacial lakes beneath the formerly more extensive Antarctic Ice Sheet. Many of the offshore basins have similar dimensions to subglacial lakes occupying bedrock depressions elsewhere in Antarctica (e.g. Wright and Siegert, 2012; Fig. 7). The elongate dimensions of the basins, aligned with the direction of former ice flow, are consistent with a glacially-

scoured origin, similar to other areas beneath the contemporary Antarctic Ice Sheet (Alley et al., 2006; Livingstone et al., 2012). For example, the offshore basins are ~2.1 times as long as they are wide, whereas glacial overdeepenings beneath the contemporary ice sheet are typically 3.3 times as long as they are wide (Patton et al., 2016).

Several studies have suggested that the basins offshore of the present-day ice-sheet margin contained subglacial lakes in the past. Analysis of sediments recovered from a basin in Pine Island Bay led Kuhn et al. (2017) to suggest that the sediments were deposited in a low energy freshwater environment; conditions that are consistent with the presence of a former subglacial lake. Furthermore, based on analysis of sediment grain size distribution, radiocarbon dating and ^{210}Pb dating, Witus et al. (2014) interpreted the uppermost sediment layer in Pine Island Bay as a meltwater plume deposit and suggested that this unit reflects episodes of meltwater discharge from subglacial basins during the late stages of ice-sheet retreat in this area. Within the Anvers-Hugo Trough, Domack et al. (2006) interpreted the network of anastomosing channels to the east of the Palmer Deep Outlet Sill to be the erosional remnant of a relict lake delta linked to the development and drainage of a subglacial lake situated in the Palmer Deep Basin, as first proposed by Rebesco et al. (1998). Seismic-reflection data indicate that the Palmer Deep Basin is infilled by a total of approximately 270 m of unconsolidated sediments, the deepest layers of which may potentially predate the Last Glacial Maximum (Rebesco et al., 1998). The great depth and relatively narrow (~2:1 length-width ratio) geometry of the basin would prevent filling by ice as the grounded margin advanced to cover the bedrock depression. Subglacial sediment deposition could then occur within the ice-free subglacial cavity by the rainout of fine-grained sediments from basal melting and lateral gravity flows triggered by the inflow of meltwater through the bedrock channels, a process which is suggested to occur for lakes beneath the contemporary ice sheet (Oswald and Robin, 1973; Shoemaker, 1991; Rebesco et al., 1998; Bentley et al., 2011; Smith et al., 2018). It is important to note, however, that whilst many of the offshore basins share similar areal dimensions to active subglacial lakes observed beneath the contemporary ice sheet, the volume of water stored in these basins would be far larger than the amount stored in contemporary actively draining subglacial lakes due to their much greater water depths (several tens to hundreds of metres). For example, Subglacial Lake Whillans has similar dimensions to many of the larger lakes identified offshore (Fig. 7), yet has a maximum depth of <8 m (Horgan et al., 2012). The filling and draining of the offshore lakes would have therefore occurred over longer timescales than implied by contemporary observations, and released larger quantities of water.

Along the margins and beneath the present-day ice sheet, geomorphological mapping and radio-echo sounding investigations have also revealed the presence of major channel features formed by subglacial meltwater. Channels that have similar dimensions to those in the western Antarctic Peninsula and Amundsen Sea (~2.6 km wide and ~160 m deep) are present along the region dividing the Möller and Foundation ice streams (Rose et al., 2014). Additional features, attributed to the action of pressurised subglacial meltwater because of their overdeepened longitudinal profiles, have been observed along the East Antarctic Ice Sheet's Soya Coast (Sawagaki and Hirakawa, 1997), within the Wilkes Subglacial Basin (Jordan et al., 2010) and at three locations in the McMurdo Dry Valleys (Sugden et al., 1991, 1999; Denton and Sugden, 2005; Lewis et al., 2006). Jordan et al. (2010) estimated the peak bankfull discharges for the channel system present in the Wilkes Subglacial Basin to be ~4.92×10^6 m^3 s^{-1} and suggested that the huge volume of water required to sustain such an outburst flood could have been sourced from an 850 km^3 subglacial lake occupying the confined central basin of this area. Similarly, in the McMurdo Dry Valleys, Lewis et al. (2006) calculated that a discharge of 1.6–2.2 $\times 10^6$ m^3 s^{-1} was associated with channel formation based on the dimensions of imbricated clasts within the channels.

Despite having statistically indistinguishable morphological characteristics (Figs. 5, 8), there appears to be a regional difference between the physical dimensions of the channels in the Amundsen Sea sector, which are larger than those in the western Antarctic Peninsula on average (Table 2). One explanation for this discrepancy is the different catchment sizes of the glaciers that extended onto the continental shelf during previous glaciations. Presently, the area of ice flowing into Pine Island Bay (~400,000 km^2) and the Dotson-Getz troughs (~110,000 km^2) is over an order of magnitude larger than the Marguerite Bay catchment (~25,000 km^2) and two orders of magnitude greater than that of the Anvers-Hugo Trough (~6000 km^2) (Cook et al., 2012; Bliss et al., 2013; Fretwell et al., 2013). Although these catchments were likely reconfigured in the past due to isostatic loading of the continental shelf by the advance of palaeo-ice-stream margins, the significantly larger catchments of the Amundsen Sea glaciers would have increased the volume of meltwater available for channel generation compared to those in the western Antarctic Peninsula.

An alternative, or possibly complementary, explanation for the larger channels in the Amundsen Sea is the influence of subglacial volcanism. The West Antarctic Ice Sheet lies over a continental rift that was active until the middle Miocene (Granot and Dyment, 2018) and is characterised by an elevated geothermal heat flux (Blankenship et al., 1993; Shapiro and Ritzwoller, 2004; Corr and Vaughan, 2008; Clow et al., 2012; LaMasurier, 2013; Fisher et al., 2015; de Vries et al., 2017; Loose et al., 2018). The hinterland of the Amundsen Sea region contains numerous volcanoes, one of which erupted as recently as ~2200 years ago (Corr and Vaughan, 2008). Furthermore, Dziadek et al. (2017, 2019) and Schroeder et al. (2014) have found indications of geothermal heat flow possibly related to young volcanic activities in this area. Analogues from Iceland demonstrate that subglacial volcanic eruptions can lead to the production of jökulhlaup outburst floods with discharges up to ~5×10^4 m^3 s^{-1} that are capable of being sustained over multiple days (Nye, 1976; Roberts, 2005). Whilst some parts of the Antarctic Peninsula also contain volcanoes and are characterised by relatively high geothermal heat fluxes (Eagles et al., 2009; Bingham et al., 2012; Martos et al., 2017), the particularly high concentration of large volcanoes in the hinterland of the Amundsen Sea region potentially explains the subtle tendency for the channels in the Amundsen Sea region to exhibit larger characteristic widths, depths, and cross-sectional areas compared to those in the western Antarctic Peninsula.

The bedrock substrate comprising the seafloor of the western Amundsen Sea Embayment is considered to be mainly granitic in composition (Smith et al., 2009b; Kipf et al., 2012; Nitsche et al., 2013), whilst the inner western Peninsula continental shelf is composed of rugged crystalline, sedimentary and volcanic rocks (Larter et al., 1997; Anderson and Oakes-Fretwell, 2008; Livingstone et al., 2013). Both regions would therefore be highly resistant to meltwater erosion (Smith et al., 2009b). Sub-bottom profiler investigations of seafloor composition within the study regions (e.g. Ó Cofaigh et al., 2005; Rackebrandt, 2006) demonstrate that unconsolidated, mainly fine-grained, sediment cover on the inner shelf is generally thin where present (<5 m), although isolated pockets of unconsolidated sediment 10–40 m thick have been observed in some channels and basins (Smith et al., 2009b; Nitsche et al., 2013; Kuhn et al., 2017). Other channels are devoid of unconsolidated sediment (Nitsche et al., 2013). Where present, sediment samples obtained from the channels in Marguerite Bay are similar to cores recovered by Smith et al. (2009b) in the Dotson-Getz trough system in the western Amundsen Sea Embayment (Hogan et al., 2016). These cores did not capture any sediments deposited by high energy meltwater processes, but acquired a sequence of glacial diamictons deposited below or close to grounded ice, overlain by unconsolidated glaciomarine muds that have been interpreted as reflecting the seasonally open-marine conditions of the present interglacial (Smith et al., 2009b). Graded sand and gravel deposits attributed to short-lived outbursts of subglacial water were recovered in a single core (site PC46) in Pine Island Bay by Lowe and Anderson (2003), although it is possible that this sequence could also reflect a turbidite deposit (Smith et al., 2009b). Poor sediment recovery rates and scratched core barrels

experienced elsewhere in Pine Island Bay led Lowe and Anderson (2003) to suggest that loose gravels may be present more widely in this area.

The presence of glacial diamictons within the base of some channels, combined with their large dimensions, suggests that these features were overridden by wet-based ice prior to the last deglacial period and are therefore likely to be significantly older than the last glaciation (Lowe and Anderson, 2003; Smith et al., 2009b). These long formation timescales are supported by numerical simulations of bedrock erosion by subglacial water flow (Beaud et al., 2018), which demonstrate that even discharges capable of transporting coarse bedload (60–500 mm particle diameter) repeated frequently over 7500 years lead to the erosion of channels that are ~20 m deep and ~100 m wide. This is substantially smaller than the mean sizes of channels on the Antarctic inner continental shelf (330–570 m wide and 37–50 m deep; Table 2). The channels were therefore probably formed progressively by numerous advances and retreats of grounded ice sheets over multiple glacial cycles (Lowe and Anderson, 2003; Smith et al., 2009b; Nitsche et al., 2013; Kirkham et al., 2019). The history of erosional overdeepening of the inner shelf areas bordering West Antarctica, however, makes it unlikely that the channels observed today are relict features formed millions of years ago at a time when ice sheets on West Antarctica were more temperate. Rapid accumulation of terrigenous sediments on the continental rise along the West Antarctic margin during the late Miocene and early Pliocene suggests that this was when overdeepening of the continental shelf occurred as a result of glacial erosion (Barker and Camerlenghi, 2002; Scheuer et al., 2006; Bart and Iwai, 2012), particularly in cross-shelf troughs where modern water depths locally exceed 1600 m. Accordingly, the sea bed within the inner shelf parts of these troughs was probably steadily overdeepened by erosion throughout the late Miocene and Pliocene, and therefore the channels cut into these surfaces must have formed more recently.

The fact that some channels contain abundant sediments whilst others do not is an indication that not all of the channels were active contemporaneously and therefore possess different histories of flow (Nitsche et al., 2013). One potential explanation for this is that, when overlain by grounded ice, some channels may remain blocked by ice until sufficient subglacial water pressure accumulates to facilitate flow into other areas of the bed (Nitsche et al., 2016). The differential blocking of some channels by varying configurations of grounded ice over multiple glacial cycles would result in the channels being exposed to different histories of subglacial water flow over time, which may contribute to the spread in channel metrics (Figure 5). The meltwater routing pathways may therefore have been spatially inconsistent between different glacial periods.

The substantial dimensions of the channels reflect the cumulative erosion of pre-existing channels inherited from previous glaciations, facilitated by the great preservation potential of bedrock to direct glacial erosion (Graham et al., 2009). The inclination for channels to tend towards a characteristic *b*-value and form ratio as they enlarge suggests that the oldest channels develop an equilibrium geometry as they are repeatedly occupied by subglacial meltwater, infilled with sediment, and overridden by ice over multiple glacial cycles. The oldest, and therefore intuitively the largest, channels will be exposed to the re-sculpting of the top of the channels by the action of glacial ice (Jørgensen and Sandersen, 2006; Jordan et al., 2010; Kirkham et al., 2019). When combined with the incision by subglacial meltwater flow at the base of the channels, this ice overriding would result in the production of a characteristic cross-sectional geometry comprising an enlarged U-shaped upper channel portion and a V-shaped lower portion, generating the characteristically low form ratios and *b*-values of ~1.1 (Larter et al., 2019).

The shape of the channels is likely to be influenced by the degree of sediment infill; this may explain some of the variation in channel *b*-values (Fig. 5) (Smith et al., 2009b; Nitsche et al., 2013). The upper sedimentary facies in Pine Island Bay consists of a well-sorted silt-rich mud drape which increases in thickness towards the modern grounding line (Kirshner et al., 2012). Witus et al. (2014) suggested that the total volume of this drape, 120 km^3, was deposited over the last ~7–8 thousand years by the episodic purging of large amounts of sediment-laden water from subglacial basins as the West Antarctic Ice Sheet retreated, with the most recent period of deposition beginning <100 years ago. Similar sediment facies have been sampled in Marguerite Bay and in the western Ross Sea, deposited concurrently with periods of rapid ice-sheet retreat in these sectors (Kennedy and Anderson, 1989; Simkins et al., 2017; Prothro et al., 2018). The sediments which make up the drape were likely expelled from the grounding zone and broadcast widely by meltwater plumes, similar to modern processes that have been observed to accelerate ice-shelf melting at the fringes of the contemporary ice sheet (e.g. Bronselaer et al., 2018; Wei et al., 2020). Although the bedrock channels in the Amundsen Sea and western Antarctic Peninsula significantly predate the formation of this drape, the extensive volume of these plumite sediments suggests that the subglacial hydrological system upstream of the bedrock channels has continued to expel large amounts of sediment laden meltwater beneath the ice sheet in relatively recent times — potentially continuing to excavate signatures of meltwater into the bed of the contemporary ice sheet.

5.3. Water transport beyond the bedrock channels

With the exception of several infilled channels that have been observed buried beneath soft sediments in the Anvers-Hugo Trough (Larter et al., 2019) and the sedimentary channels present in the Ross Sea (Simkins et al., 2017), meltwater channels are generally absent from the softer sediments present on the middle and outer continental shelves around Antarctica (Fig. 2). This discrepancy suggests that the transport of subglacial meltwater may have halted, or operated via a different mechanism, beyond the transition to the softer middle and outer shelf sediments. Glacimarine sediment deposition from subglacial meltwater streams (emitted from an ice margin) produces well-sorted sedimentary sequences that are sorted into finer fractions with distance from the outlet point (Powell, 1990; Mugford and Dowdeswell, 2011; Dowdeswell et al., 2015). The absence of depositional sedimentary fans at the bedrock-sedimentary transition imaged in the multibeam bathymetry data analysed here implies that the flow of meltwater transported through the inner-shelf channel network did not simply terminate abruptly at this transition.

It is notable that, to the best of our knowledge, no tunnel valleys exist seaward of the bedrock channels where sedimentary strata occur in the Amundsen Sea and western Antarctic Peninsula. Tunnel valleys are large sedimentary channels incised by pressurised subglacial meltwater (e.g. Huuse and Lykke-Andersen, 2000; Cutler et al., 2002; Jørgensen and Sandersen, 2006; Boulton et al., 2007; Kehew et al., 2012; van der Vegt et al., 2012). They are common in sedimentary sequences in northwest Europe (e.g. Ehlers et al., 1984; Praeg, 2003; Jørgensen and Sandersen, 2006; Kristensen et al., 2007, 2008; Sandersen et al., 2009; Hepp et al., 2012; Stewart et al., 2013), Australia (Eyles and de Broekert, 2001), North America (Atkinson et al., 2013; MacRae and Christians, 2013; Pugin et al., 2014), northwest Africa (Ghienne and Deynoux, 1998; Denis et al., 2007; Ravier et al., 2015) and in the Baltic and Barents seas (Greenwood et al., 2016; Bjarnadóttir et al., 2017). Tunnel valleys possess many of the same characteristics as the bedrock channels analysed on Antarctic inner continental shelves, including similar dimensions (Fig. 9), undulating longitudinal profiles and steep-sided cross sections that are typically 10–20 times wider than they are deep (Huuse and Lykke-Andersen, 2000; Kristensen et al., 2007; Stewart et al., 2013). In some locations such as the North Sea, it is possible to separate the tunnel valleys into cross cutting generations that can be tentatively correlated to individual glacial cycles; this implies that it is possible for subglacial meltwater to erode channels several kilometres wide and hundreds of metres deep within one glacial period (Stewart and Lonergan, 2011; Stewart et al., 2013),

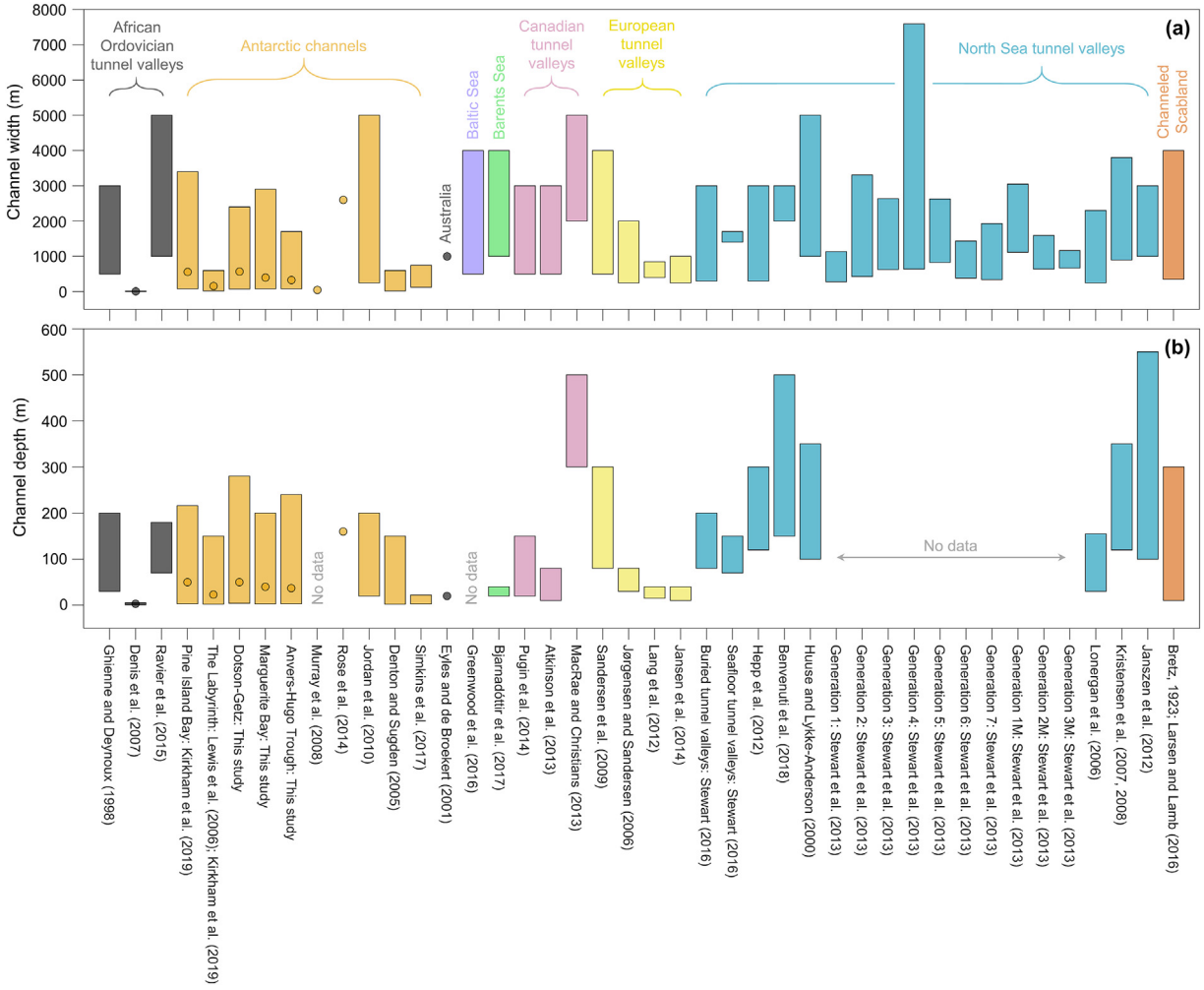

Fig. 9. Comparison of the range of channel widths and depths observed around Antarctica with other formerly glaciated regions. Bars display the minimum to maximum range of channel widths and depths reported in the literature. Where reported, mean channel widths and depths are shown as coloured dots.

albeit in much softer substrates than present on the Antarctic inner continental shelf.

Sediment infill analysis (Lowe and Anderson, 2003; Smith et al., 2009b; Hogan et al., 2016), combined with numerical simulations of subglacial water flow through bedrock channels (e.g. Beaud et al., 2018; Kirkham et al., 2019) suggests that such high rates of erosion did not occur for the channels on the Antarctic continental shelf. This discrepancy may be explained by the incision of the tunnel valleys into relatively soft sediments compared to often overconsolidated glacial till or bedrock (Passchier et al., 2010), as well as greater water availability from surface melt which likely drained to the ice sheet bed in many of the lower latitude settings where tunnel valleys are present (e.g. Carlson et al., 2008; Jansen et al., 2014). The most similar Antarctic features to the buried tunnel valleys found in other regions were reported by Montelli et al. (2019) on the Sabrina Coast shelf of East Antarctica. There, buried channels up to 1150 m wide are present on erosional surfaces dated to the Late Eocene to Late Miocene, indicating the presence of temperate, meltwater rich glaciations in the Aurora Basin catchment (Montelli et al., 2019). The formation of these tunnel valleys likely predates the bedrock channels in the Amundsen Sea and western Antarctic Peninsula as numerical models suggest that the West Antarctic Ice Sheet was not sufficiently developed at this time to allow large scale grounded ice to extend onto the inner continental shelves of these regions (DeConto and Pollard, 2003). Overall, the size, shape, and form of the bedrock channels present on the Antarctic inner continental shelf are similar to channels eroded into the substrate of other formerly glaciated regions. The formative process responsible for these features may therefore be genetically related, although further work is required to constrain the timescales and the portion of a glacial cycle in in which channel incision is most prevalent.

With the absence of further channelised drainage systems seaward of the bedrock channels, several other possible explanations exist to explain how water may have moved beyond the bedrock-sediment transition. Meltwater could have been evacuated via a canalised drainage system similar to those observed and predicted under contemporary ice streams (Walder and Fowler, 1994; Ng, 2000; Murray et al., 2008; Schroeder et al., 2013) or via Darcian flow through the unconsolidated sediments themselves, notably since subglacial tills exhibit a higher permeability than the acoustic basement of the inner shelf (Graham et al., 2009). The relatively delicate morphological signatures associated with these distributed drainage systems would be unlikely to survive reworking by the action of overriding ice as soon as any canalised drainage system became inactive. This could have occurred during full glacial conditions for features on the outermost shelf, or during ice retreat where till deformation at the bed probably would have obliterated any evidence of channelised flow (Nitsche et al., 2013). It is also possible that more channels exist buried beneath soft sediments that were not reworked by the next advance of grounded ice, similar to those described by Larter et al. (2019). The scale of these features may be below the resolution of conventional seismic data, and thus a dense

grid of high-resolution seismic data seaward of the bedrock channels would be required to explore this hypothesis.

6. Conclusions

Geomorphological records of past channel systems and possible subglacial lakes revealed on deglaciated continental shelves provide insights into inaccessible modern subglacial hydrological processes which may not be captured by contemporary glaciological observations. Utilising multibeam bathymetric data collected over the past two decades and covering an area of over 100,000 km^2, this study represents the most complete existing inventory of submarine channel features present on the West Antarctic continental shelf. Quantitative morphometric analysis of the bedrock channel features has permitted, for the first time, the geomorphological characteristics of over 2700 individual channels to be derived and compared between four different continental shelf regions. Channels range between 75 and 3400 m in width, are 3–280 m deep, and typically exhibit V-shaped channel cross sections that are eight times as wide as they are deep, with cross-sectional areas of 160–290,000 m^2.

The bifurcating and anastomosing structure of the bedrock channel systems, combined with their undulating thalwegs, imply that they were eroded by pressurised subglacial meltwater flowing under the formerly expanded outlets of the Antarctic Ice Sheet. The channels have similar dimensions and shapes to tunnel valleys incised into soft sediments in other formerly glaciated regions. However, whilst many tunnel valleys have been suggested to form in one glacial cycle, the tendency for the Antarctic channels to converge towards an equilibrium geometry as they enlarge, combined with their incision into bedrock, suggests that they are composite features produced by incision into bedrock over multiple glacial cycles. The channel assemblages present in the western Antarctic Peninsula are smaller on average compared to those observed in the Amundsen Sea. This difference is probably related to regional order-of-magnitude differences in glacier catchment area, and the production of additional meltwater through volcanic activity and an elevated geothermal heat flux in the Amundsen Sea region.

The abundance and great spatial extent over which the submarine channels are observed suggests that, when active, the palaeohydrological system of the Antarctic Ice Sheet has been characterised at one or more times in the past by an abundance of subglacial meltwater. Such an interpretation is inconsistent with the subglacial hydrological system believed to be present under the contemporary Antarctic Ice Sheet if channelised meltwater flow is assumed to be continuous. Instead, the water responsible for generating the channels mapped in this study was most likely sourced from the episodic drainage of former subglacial lakes. Each of the regions examined here contains basin-like depressions that are distinguishable from the meltwater channels through their significantly greater areal dimensions, steep bounding sides, and the incidence of subdued geomorphic features on the flat basin floors. Geomorphological, seismic and sedimentological evidence suggests that these depressions were formerly subglacial lakes occupying glacially-scoured basins. Episodic discharges from these subglacial lakes would have provided sufficient water and sediment to incise the channels observed on the Antarctic inner continental shelf when repeated over multiple glacial cycles.

Declaration of competing interest

The authors declare no competing interests.

Acknowledgements

We thank the masters and crews of the research vessels, RVIB *Nathaniel B. Palmer*, RRS *James Clark Ross*, RV *Polarstern*, RV *Maurice Ewing*, HMS *Endurance*, HMS *Scott* and HMS *Protector* for their support during data acquisition. Bathymetry data from the expedition ANT-XXIII/4 (Schenke et al., 2008) and ANT-XXVI/3 (Gohl, 2010) were provided courtesy of the bathymetry group at the Geophysics Section, Alfred Wegener Institute, Helmholtz Centre for Polar and Marine Research (AWI). We thank Povl Abrahamsen (BAS) for helping to initially clean the iSTAR bathymetry data, James Smith (BAS) for insightful discussions about the sedimentology of the channels, and two anonymous reviewers for helpful comments that improved the paper.

Funding

This work was supported by the UK Natural Environment Research Council (NERC) [grant number NE/L002507/1]; a Debenham Scholarship from the Scott Polar Research Institute, University of Cambridge; the NERC – British Antarctic Survey Polar Science for Planet Earth programme; and the Alfred Wegener Institute, Helmholtz Centre for Polar and Marine Research programme: Polar Regions and Coasts in the changing Earth System (PACES II). Some of the data used were collected through other projects [NERC grant numbers NE/J005703/1, NE/J005746/1, NE/J005770/1 and National Science Foundation grant 0838735].

Data availability

Marine geophysical data are available on request to the UK Polar Data Centre (https://www.bas.ac.uk/data/uk-pdc/, last access: 9 July 2019) and the National Centers for Environmental Information (https://www.ngdc.noaa.gov/mgg/bathymetry/multibeam.html, last access: 9 July 2019) for RRS *James Clark Ross* and RVIB *Nathaniel B. Palmer* data, respectively, and on request via PANGAEA (https://pangaea.de/, last access: 9 July 2019) for RV *Polarstern* data. Datasets analysed during the study are available upon reasonable request to the corresponding author.

Author contributions

Robert D. Larter, Julian A. Dowdeswell and Kelly A. Hogan conceived the study; they and Frank O. Nitsche, Gerhard Kuhn, Karsten Gohl, and John B. Anderson participated in cruises to collect the data. James D. Kirkham analysed the bathymetry data and conducted the channel measurements. James D. Kirkham wrote the initial paper with contributions from Kelly A. Hogan, Julian A. Dowdeswell and Robert D. Larter. All authors contributed to data interpretation and writing of the final paper.

References

Alley, R.B., Anandakrishnan, S., Bentley, C.R., Lord, N., 1994. A water-piracy hypothesis for the stagnation of Ice Stream C, Antarctica. Ann. Glaciol. 20 (1), 187–194. https://doi.org/10.1017/S0260305500016438.

Alley, R.B., Cuffey, K.M., Evenson, E.B., Strasser, J.C., Lawson, D.E., Larson, G.J., 1997. How glaciers entrain and transport basal sediment: physical constraints. Quat. Sci. Rev. 16, 1017–1038. https://doi.org/10.1016/S0277-3791(97)00034-6.

Alley, R.B., Dupont, T.K., Parizek, B.R., Anandakrishnan, S., Lawson, D.E., Larson, G.J., Evenson, E.B., 2006. Outburst flooding and the initiation of ice-stream surges in response to climatic cooling: a hypothesis. Geomorphology. 75 (1), 76–89. https://doi.org/10.1016/j.geomorph.2004.01.011.

Anandakrishnan, S., Blankenship, D.D., Alley, R.B., Stoffa, P.L., 1998. Influence of subglacial geology on the position of a West Antarctic ice stream from seismic observations. Nature 394 (6688), 62–65. https://doi.org/10.1038/27889.

Anandakrishnan, S., Alley, R.B., Jacobel, R., Conway, H., 2001. The flow regime of Ice Stream C and hypotheses concerning its recent stagnation. In: Alley, R.B., Bindschadler, R.A. (Eds.), The West Antarctic Ice Sheet: Behavior and Environment. Antarctic Research Series 77. AGU, Washington, DC, pp. 283–296. https://doi.org/10.1029/AR077p0283.

Anderson, J.B., Oakes-Fretwell, L., 2008. Geomorphology of the onset area of a paleo-ice stream, Marguerite Bay, Antarctic Peninsula. Earth Surf. Process. Landf. 33 (4), 503–512. https://doi.org/10.1002/esp.1662.

Anderson, J.B., Shipp, S.S., Lowe, A.L., Wellner, J.S., Mosola, A.B., 2002. The Antarctic Ice Sheet during the Last Glacial Maximum and its subsequent retreat history: a review. Quat. Sci. Rev. 21 (1), 49–70. https://doi.org/10.1016/S0277-3791(01)00083-X.

Arndt, J.E., Schenke, H.-W., Jakobsson, M., Nitsche, F.O., Buys, G., Goleby, B., Rebesco, M., Bohoyo, F., Hong, J.K., Black, J., Greku, R., Udintsev, G., Barrios, F., Reynoso-Peralta,

W., Taisei, M., Wigley, R., 2013. The International Bathymetric Chart of the Southern Ocean (IBCSO) Version 1.0 - a new bathymetric compilation covering circum-Antarctic waters. Geophys. Res. Lett. 40, 3111–3117. https://doi.org/10.1002/grl.50413.
Ashmore, D.W., Bingham, R.G., 2014. Antarctic subglacial hydrology: current knowledge and future challenges. Antarct. Sci. 26 (6), 758–773. https://doi.org/10.1017/S0954102014000546.
Atkinson, N., Andriashek, L.D., Slattery, S.R., 2013. Morphological analysis and evolution of buried tunnel valleys in northeast Alberta, Canada. Quaternary Science Reviews. 65, 53–72. https://doi.org/10.1016/j.quascirev.2012.11.031.
Barker, P.F., Camerlenghi, A., 2002. Glacial history of the Antarctic Peninsula from Pacific margin sediments. In: Barker, P.F., Camerlenghi, A., Acton, G.D., Ramsay, A.T.S. (Eds.), Proc. ODP, Sci. Results, 178 [Online] Available http://www-odp.tamu.edu/publications/178_SR/synth/synth.htm.
Bart, P.J., 2001. Did the Antarctic ice sheets expand during the early Pliocene? Geology. 29 (1), 67–70. https://doi.org/10.1130/0091-7613(2001)029<0067:DTAISE>2.0.CO;2.
Bart, P.J., 2003. Were West Antarctic Ice Sheet grounding events in the Ross Sea a consequence of East Antarctic Ice Sheet expansion during the middle Miocene? Earth Planet Science Letters. 216, 1–2. https://doi.org/10.1016/S0012-821X(03)00509-0.
Bart, P.J., Anderson, J.B., 1995. Seismic record of glacial events affecting the Pacific margin of the northwestern Antarctic Peninsula. In: Cooper, A.K., Barker, P.F., Brancolini, G. (Eds.), Geology and Seismic Stratigraphy of the Antarctic Margin. Antarctic Research Series 68, pp. 75–95.
Bart, P.J., Iwai, M., 2012. The overdeepening hypothesis: how erosional modification of the marine-scape during the early Pliocene altered glacial dynamics on the Antarctic Peninsula's Pacific margin. Palaeogeogr. Palaeoclimatol. Palaeoecol. 335, 42–51. https://doi.org/10.1016/j.palaeo.2011.06.010.
Bart, P. J., Egan, D., Warny, S. A., 2005. Direct constraints on Antarctic Peninsula Ice Sheet grounding events between 5.12 and 7.94 Ma. Journal of Geophysical Research. 110, F04008, https://doi.org/10.1029/2004JF000254.
Bartholomew, I., Nienow, P., Sole, A., Mair, D., Cowton, T., King, M.A., 2012. Short-term variability in Greenland Ice Sheet motion forced by time-varying meltwater drainage: implications for the relationship between subglacial drainage system behavior and ice velocity. Journal of Geophysical Research: Earth Surface. 117 (F3). https://doi.org/10.1029/2011JF002220.
Batchelor, C.L., Dowdeswell, J.A., 2014. The physiography of High Arctic cross-shelf troughs. Quat. Sci. Rev. 92, 68–96. https://doi.org/10.1016/j.quascirev.2013.05.025.
Beaud, F., Venditti, J.G., Flowers, G.E., Koppes, M., 2018. Excavation of subglacial bedrock channels by seasonal meltwater flow. Earth Surf. Process. Landf. 43 (9), 1960–1972. https://doi.org/10.1002/esp.4367.
Bell, R.E., 2008. The role of subglacial water in ice-sheet mass balance. Nat. Geosci. 1 (5), 297–304. https://doi.org/10.1038/ngeo186.
Bell, R.E., Chu, W., Kingslake, J., Das, I., Tedesco, M., Tinto, K.J., Zappa, C.J., Frezzotti, M., Boghosian, A., Lee, W.S., 2017. Antarctic ice shelf potentially stabilized by export of meltwater in surface river. Nature. 544 (7650), 344–348. https://doi.org/10.1038/nature22048.
Bell, R.E., Banwell, A.F., Trusel, L.D., Kingslake, J., 2018. Antarctic surface hydrology and impacts on ice-sheet mass balance. Nat. Clim. Chang. https://doi.org/10.1038/s41558-018-0326-3.
Bentley, M.J., Christoffersen, P., Hodgson, D.A., Smith, A.M., Tulaczyk, S., Le Brocq, A.M., 2011. Subglacial lake sediments and sedimentary processes: potential archives of ice sheet evolution, past environmental change, and the presence of life. In: Siegert, M.J., Kennicutt III, M.C., Bindschadler, R.A. (Eds.), Antarctic Subglacial Aquatic Environments, Geophysical Monograph Series, 192. American Geophysical Union, Washington DC, pp. 83–110 https://doi.org/10.1029/2010GM000940.
Bindschadler, R., Choi, H., 2007. Increased water storage at ice-stream onsets: a critical mechanism? J. Glaciol. 53 (181), 163–171. https://doi.org/10.3189/172756507782202793.
Bingham, R.G., Ferraccioli, F., King, E.C., Larter, R.D., Pritchard, H.D., Smith, A.M., Vaughan, D.G., 2012. Inland thinning of West Antarctic Ice Sheet steered along subglacial rifts. Nature. 487 (7408), 468–471. https://doi.org/10.1038/nature11292.
Bjarnadóttir, L.R., Winsborrow, M.C.M., Andreassen, K., 2017. Large subglacial meltwater features in the central Barents Sea. Geology. 45, 159–162. https://doi.org/10.1130/G38195.1.
Björnsson, H., 2002. Subglacial lakes and jökulhlaups in Iceland. Glob. Planet. Chang. 35 (3), 255–271. https://doi.org/10.1016/S0921-8181(02)00130-3.
Blankenship, D.D., Bell, R.E., Hodge, S.M., Brozena, J.M., Behrendt, J.C., Finn, C.A., 1993. Active volcanism beneath the West Antarctic ice sheet and implications for ice-sheet stability. Nature. 361, 526–529. https://doi.org/10.1038/361526a0.
Bliss, A., Hock, R., Cogley, J.G., 2013. A new inventory of mountain glaciers and ice caps for the Antarctic periphery. Ann. Glaciol. 54 (63), 191–199. https://doi.org/10.3189/2013AoG63A377.
Bougamont, M., Christoffersen, P., Nias, I., Vaughan, D.G., Smith, A.M., Brisbourne, A., 2019. Contrasting hydrological controls on bed properties during the acceleration of Pine Island Glacier, West Antarctica. Journal of Geophysical Research: Earth Surface 124, 80–96. https://doi.org/10.1029/2018JF004707.
Boulton, G.S., Caban, P.E., Van Gijssel, K., 1995. Groundwater flow beneath ice sheets: part I—large scale patterns. Quat. Sci. Rev. 14 (6), 545–562. https://doi.org/10.1016/0277-3791(95)00039-R.
Boulton, G.S., Lunn, R., Vidstrand, P., Zatsepin, S., 2007. Subglacial drainage by groundwater-channel coupling, and the origin of esker systems: part 1—glaciological observations. Quat. Sci. Rev. 26 (7–8), 1067–1090. https://doi.org/10.1016/j.quascirev.2007.01.007.
Bretz, J.H., 1923. The channeled scablands of the Columbia Plateau. The Journal of Geology. 31 (8), 617–649. https://doi.org/10.1086/623053.
Bronselaer, B., Winton, M., Griffies, S.M., Hurlin, W.J., Rodgers, K.B., Sergienko, O.V., Stouffer, R.J., Russell, J.L., 2018. Change in future climate due to Antarctic meltwater. Nature. 564, 53–58. https://doi.org/10.1038/s41586-018-0712-z.
Caress, D.W., Chayes, D.N., 2004. MB-System version 5. Open Source Software Distributed From the MBARI and L-DEO Web Sites.
Caress, D. W., Chayes, D. N., and Ferreira, C. 2020. MB-System Seafloor Mapping Software, available at: https://www.mbari.org/products/research-software/mb-system/, last access: 20/08/2020.
Carlson, A.E., LeGrande, A.N., Oppo, D.W., Came, R.E., Schmidt, G.A., Anslow, F.S., Licciardi, J.M., Obbink, E.A., 2008. Rapid early Holocene deglaciation of the Laurentide ice sheet. Nat. Geosci. 1, 620–624. https://doi.org/10.1038/ngeo285.
Carter, S.P., Blankenship, D.D., Peters, M.E., Young, D.A., Holt, J.W., Morse, D.L., 2007. Radar-based subglacial lake classification in Antarctica. *Geochemistry, Geophysics, Geosystems. 8*(3). https://doi.org/10.1029/2006GC001408
Chow, J.M., Bart, P.J., 2003. West Antarctic Ice Sheet grounding events on the Ross Sea outer continental shelf during the middle Miocene. Palaeogeogr. Palaeoclimatol. Palaeoecol. 198, 169–186. https://doi.org/10.1016/S0031-0182(03)00400-0.
Christoffersen, P., Bougamont, M., Carter, S.P., Fricker, H.A., Tulaczyk, S., 2014. Significant groundwater contribution to Antarctic ice streams hydrologic budget. Geophys. Res. Lett. 41 (6), 2003–2010. https://doi.org/10.1002/2014GL059250.
Cirillo, P., 2013. Are your data really Pareto distributed? Physica A: Statistical Mechanics and its Applications. 392 (23), 5947–5962. https://doi.org/10.1016/j.physa.2013.07.061.
Clark, C.D., 1993. Mega-scale glacial lineations and cross-cutting ice-flow landforms. Earth Surf. Process. Landf. 18 (1), 1–29. https://doi.org/10.1002/esp.3290180102.
Clow, G.D., Cuffey, K.M., Waddington, E.D., 2012. December. High heat-flow beneath the central portion of the West Antarctic Ice Sheet. AGU Fall Meeting Abstract. Available: https://ui.adsabs.harvard.edu/abs/2012AGUFM.C31A0577C/abstract.
Cook, A.J., Murray, T., Luckman, A., Vaughan, D.E., Barrand, N.E., 2012. A new 100-m Digital Elevation Model of the Antarctic Peninsula derived from ASTER Global DEM: methods and accuracy assessment. Earth System Science Data. 4 (1), 129–142. https://doi.org/10.5194/essd-4-129-2012.
Cook, C.P., Van De Flierdt, T., Williams, T., Hemming, S.R., Iwai, M., Kobayashi, M., Jimenez-Espejo, F.J., Escutia, C., González, J.J., Khim, B.K., McKay, R.M., 2013. Dynamic behaviour of the East Antarctic ice sheet during Pliocene warmth. Nat. Geosci. 6 (9), 765–769. https://doi.org/10.1038/ngeo1889.
Corr, H.F., Vaughan, D.G., 2008. A recent volcanic eruption beneath the West Antarctic ice sheet. Nat. Geosci. 1 (2), 122–125. https://doi.org/10.1038/ngeo106.
Cowton, T., Nienow, P., Bartholomew, I., Sole, A., Mair, D., 2012. Rapid erosion beneath the Greenland ice sheet. Geology. 40, 343–346. https://doi.org/10.1130/G32687.1.
Craig, C.C., 1936. A new exposition and chart for the Pearson system of frequency curves. Ann. Math. Stat. 7, 16–28. https://doi.org/10.1214/aoms/1177732542.
Cutler, P.M., Colgan, P.M., Mickelson, D.M., 2002. Sedimentologic evidence for outburst floods from the Laurentide Ice Sheet margin in Wisconsin, USA: implications for tunnel-channel formation. Quat. Int. 90 (1), 23–40. https://doi.org/10.1016/S1040-6182(01)00090-8.
Das, S.B., Joughin, I., Behn, M.D., Howat, I.M., King, M.A., Lizarralde, D., Bhatia, M.P., 2008. Fracture propagation to the base of the Greenland Ice Sheet during supraglacial lake drainage. Science. 320 (5877), 778–781. https://doi.org/10.1126/science.1153360.
de Vries, M.V.W., Bingham, R.G., Hein, A.S., 2017. A new volcanic province: an inventory of subglacial volcanoes in West Antarctica. Geol. Soc. Lond., Spec. Publ. 461, SP461–7. https://doi.org/10.1144/SP461.7.
DeConto, R.M., Pollard, D., 2003. A coupled climate–ice sheet modeling approach to the early Cenozoic history of the Antarctic ice sheet. Palaeogeogr. Palaeoclimatol. Palaeoecol. 198, 39–52. https://doi.org/10.1016/S0031-0182(03)00393-6.
Denis, M., Buoncristiani, J.F., Konaté, M., Guiraud, M., Eyles, N., 2007. The origin and glaciodynamic significance of sandstone ridge networks from the Hirnantian glaciation of the Djado Basin (Niger). Sedimentology. 54 (6), 1225–1243. https://doi.org/10.1111/j.1365-3091.2007.00879.x.
Denton, G.H., Sugden, D.E., 2005. Meltwater features that suggest Miocene ice-sheet overriding of the Transantarctic Mountains in Victoria Land, Antarctica. Geografiska Annaler: Series A, Physical Geography. 87 (1), 67–85. https://doi.org/10.1111/j.0435-3676.2005.00245.x.
Domack, E., Amblàs, D., Gilbert, R., Brachfeld, S., Camerlenghi, A., Rebesco, M., Canals, M., Urgeles, R., 2006. Subglacial morphology and glacial evolution of the Palmer deep outlet system, Antarctic Peninsula. Geomorphology. 75 (1), 125–142. https://doi.org/10.1016/j.geomorph.2004.06.013.
Domack, E.W., Amblas, D., Canals, M., 2016. Bedrock meltwater channels in Palmer Deep, Antarctic Peninsula. In: Dowdeswell, J. A., Canals, M., Jakobsson, M., Todd, B. J., Dowdeswell, E. K., Hogan, K. A. (Eds.), Atlas of Submarine Glacial Landforms: Modern, Quaternary and Ancient. Geological Society, London, Memoirs 46, 211–212. https://doi.org/10.1144/M46.52.
Dowdeswell, J.A., Siegert, M.J., 1999. The dimensions and topographic setting of Antarctic subglacial lakes and implications for large-scale water storage beneath continental ice sheets. Geol. Soc. Am. Bull. 111 (2), 254–263. https://doi.org/10.1130/0016-7606.
Dowdeswell, J.A., Siegert, M.J., 2003. The physiography of modern Antarctic subglacial lakes. Glob. Planet. Chang. 35 (3), 221–236. https://doi.org/10.1016/S0921-8181(02)00128-5.
Dowdeswell, J.A., Evans, J., Ó Cofaigh, C., 2010. Submarine landforms and shallow acoustic stratigraphy of a 400 km-long fjord-shelf-slope transect, Kangerlussuaq margin, East Greenland. Quat. Sci. Rev. 29 (25), 3359–3369. https://doi.org/10.1016/j.quascirev.2010.06.006.
Dowdeswell, J.A., Hogan, K.A., Ó Cofaigh, C., Fugelli, E.M.G., Evans, J., Noormets, R., 2014. Late Quaternary ice flow in a West Greenland fjord and cross-shelf trough system: submarine landforms from Rink Isbrae to Uummannaq shelf and slope. Quat. Sci. Rev. 92, 292–309. https://doi.org/10.1016/j.quascirev.
Dowdeswell, J.A., Hogan, K.A., Arnold, N.S., Mugford, R.I., Wells, M., Hirst, J.P.P., Decalf, C., 2015. Sediment-rich meltwater plumes and ice-proximal fans at the margins of

modern and ancient tidewater glaciers: observations and modelling. Sedimentology. 62 (6), 1665–1692. https://doi.org/10.1111/sed.12198.

Dowdeswell, J.A., Canals, M., Jakobsson, M., Todd, B.J., Dowdeswell, E.K., Hogan, K.A., 2016. The variety and distribution of submarine glacial landforms and implications for ice-sheet reconstruction. In: Dowdeswell, J. A., Canals, M., Jakobsson, M., Todd, B. J., Dowdeswell, E. K., Hogan, K. A. (Eds.), Atlas of Submarine Glacial Landforms: Modern, Quaternary and Ancient. Geological Society, London, Memoirs 46, 519–552. https://doi.org/10.1144/M46.183.

Dziadek, R., Gohl, K., Diehl, A., Kaul, N., 2017. Geothermal heat flux in the Amundsen Sea sector of West Antarctica: new insights from temperature measurements, depth to the bottom of the magnetic source estimation and thermal modelling. Geochemistry Geophysics Geosystems. 18, 2657–2672. https://doi.org/10.1002/2016GC006755.

Dziadek, R., Gohl, K., Kaul, N., Science Team of Expedition PS104, 2019. Elevated geothermal surface heat flow in the Amundsen Sea Embayment, West Antarctica. Earth and Planetary Science Letters 506, 530–539. https://doi.org/10.1016/j.epsl.2018.11.003.

Eagles, G., Larter, R.D., Gohl, K., Vaughan, A.P.M., 2009. West Antarctic Rift System in the Antarctic Peninsula. Geophys. Res. Lett. 36, L21305. https://doi.org/10.1029/2009GL040721.

Ehlers, J., Meyer, K.D., Stephan, H.J., 1984. The pre-Weichselian glaciations of north-west Europe. Quat. Sci. Rev. 3 (1), 1–40. https://doi.org/10.1016/0277-3791(84)90003-9.

Evans, J., Ó Cofaigh, C., Dowdeswell, J.A., Wadhams, P., 2009. Marine geophysical evidence for former expansion and flow of the Greenland Ice Sheet across the north-east Greenland continental shelf. J. Quat. Sci. 24 (3), 279–293. https://doi.org/10.1002/jqs.1231.

Evatt, G.W., Fowler, A.C., Clark, C.D., Hulton, N.R.J., 2006. Subglacial floods beneath ice sheets. Philosophical Transactions of the Royal Society of London A: Mat. Phys. Eng. Sci. 364 (1844), 1769–1794. https://doi.org/10.1098/rsta.2006.1798.

Eyles, N., de Broekert, P., 2001. Glacial tunnel valleys in the Eastern Goldfields of Western Australia cut below the Late Paleozoic Pilbara ice sheet. Palaeogeogr. Palaeoclimatol. Palaeoecol. 171 (1–2), 29–40. https://doi.org/10.1016/S0031-0182(01)00265-6.

Fisher, A.T., Mankoff, K.D., Tulaczyk, S.M., Tyler, S.W., Foley, N., 2015. High geothermal heat flux measured below the West Antarctic Ice Sheet. Sci. Adv. 1 (6), e1500093. https://doi.org/10.1126/sciadv.1500093.

Flament, T., Berthier, E., Rémy, F., 2014. Cascading water underneath Wilkes Land, East Antarctic ice sheet, observed using altimetry and digital elevation models. Cryosphere 8 (2), 673–687. https://doi.org/10.5194/tc-8-673-2014.

Fretwell, P., Pritchard, H.D., Vaughan, D.G., Bamber, J.L., Barrand, N.E., Bell, R., Bianchi, C., Bingham, R.G., Blankenship, D.D., Casassa, G., Catania, G., 2013. Bedmap2: improved ice bed, surface and thickness datasets for Antarctica. Cryosphere 7 (1), 375–393. https://doi.org/10.5194/tc-7-375-2013.

Fricker, H.A., Scambos, T., Bindschadler, R., Padman, L., 2007. An active subglacial water system in West Antarctica mapped from space. Science. 315 (5818), 1544–1548. https://doi.org/10.1126/science.1136897.

Gales, J.A., Larter, R.D., Mitchell, N.C., Dowdeswell, J.A., 2013. Geomorphic signature of Antarctic submarine gullies: implications for continental slope processes. Mar. Geol. 337, 112–124. https://doi.org/10.1016/j.margeo.2013.02.003.

Galofre, A.G., Jellinek, A.M., Osinski, G.R., Zanetti, M., Kukko, A., 2018. Subglacial drainage patterns of Devon Island, Canada: detailed comparison of rivers and subglacial meltwater channels. Cryosphere 12, 1461–1478. https://doi.org/10.5194/tc-12-1461-2018.

Ghienne, J.F., Deynoux, M., 1998. Large scale channel fill structures in Late Ordovician glacial deposits in Mauritania, western Sahara. Sediment. Geol. 119, 141–159. https://doi.org/10.1016/S0037-0738(98)00045-1.

Gohl, K., 2010. The Expedition of the Research Vessel "Polarstern" to the Amundsen Sea, Antarctica, in 2010 (ANT-XXVI/3). Bremerhaven: Alfred Wegener Institute for Polar and Marine Research, 169 pp. http://epic.awi.de/29635/

Gohl, K., Uenzelmann-Neben, G., Larter, R.D., Hillenbrand, C.D., Hochmuth, K., Kalberg, T., Weigelt, E., Davy, B., Kuhn, G., Nitsche, F.O., 2013. Seismic stratigraphic record of the Amundsen Sea Embayment shelf from pre-glacial to recent times: evidence for a dynamic West Antarctic ice sheet. Mar. Geol. 344, 115–131. https://doi.org/10.1016/j.margeo.2013.06.011.

Graf, W.L., 1970. The geomorphology of the glacial valley cross section. Arct. Alp. Res. 2 (4), 303–312. https://doi.org/10.2307/1550243.

Graham, A.G., Larter, R.D., Gohl, K., Hillenbrand, C.D., Smith, J.A., Kuhn, G., 2009. Bedform signature of a West Antarctic palaeo-ice stream reveals a multi-temporal record of flow and substrate control. Quat. Sci. Rev. 28 (25), 2774–2793. https://doi.org/10.1016/j.quascirev.2009.07.003.

Graham, A.G., Larter, R.D., Gohl, K., Dowdeswell, J.A., Hillenbrand, C.D., Smith, J.A., Evans, J., Kuhn, G., Deen, T., 2010. Flow and retreat of the Late Quaternary Pine Island-Thwaites palaeo-ice stream, West Antarctica. Journal of Geophysical Research: Earth Surface. 115 (F3). https://doi.org/10.1029/2009JF001482.

Granot, R., Dyment, J., 2018. Late Cenozoic unification of East and West Antarctica. Nat. Commun. 9 (1), 1–10. https://doi.org/10.1038/s41467-018-05270-w.

Greenwood, S.L., Clark, C.D., Hughes, A.L., 2007. Formalising an inversion methodology for reconstructing ice-sheet retreat patterns from meltwater channels: application to the British Ice Sheet. J. Quat. Sci. 22 (6), 637–645. https://doi.org/10.1002/jqs.1083.

Greenwood, S.L., Clason, C.C., Jakobsson, M., 2016. Ice-flow and meltwater landform assemblages in the Gulf of Bothnia. In: Dowdeswell, J. A., Canals, M., Jakobsson, M., Todd, B. J., Dowdeswell, E. K., Hogan, K. A. (Eds.), Atlas of Submarine Glacial landforms: Modern, Quaternary and Ancient. Geological Society, London, Memoirs 46, 321–324. https://doi.org/10.1144/M46.163.

Gupta, S., Collier, J.S., Palmer-Felgate, A., Potter, G., 2007. Catastrophic, flooding origin of shelf valley systems in the English Channel. Nature. 448, 342–345. https://doi.org/10.1038/nature06018.

Harbor, J.M., 1992. Numerical modeling of the development of U-shaped valleys by glacial erosion. Geol. Soc. Am. Bull. 104 (10), 1364–1375. https://doi.org/10.1130/0016-7606.

Hepp, D.A., Hebbeln, D., Kreiter, S., Keil, H., Bathmann, C., Ehlers, J., Mörz, T., 2012. An east–west-trending Quaternary tunnel valley in the south-eastern North Sea and its seismic–sedimentological interpretation. J. Quat. Sci. 27 (8), 844–853. https://doi.org/10.1002/jqs.2599.

Hernández-Molina, F.J., Larter, R.D., Maldonao, A., 2017. Neogene to Quaternary Stratigraphic Evolution of the Antarctic Peninsula, Pacific Margin offshore of Adelaide Island: transitions from a non-glacial, through glacially-influenced to a fully glacial state. Glob. Planet. Chang. 156, 80–111. https://doi.org/10.1016/j.gloplacha.2017.07.002.

Hewitt, I.J., 2013. Seasonal changes in ice sheet motion due to melt water lubrication. Earth Planet. Sci. Lett. 371, 16–25. https://doi.org/10.1016/j.epsl.2013.04.022.

Hillenbrand, C.D., Smith, J.A., Hodell, D.A., Greaves, M., Poole, C.R., Kender, S., Williams, M., Andersen, T.J., Jernas, P.E., Elderfield, H., Klages, J.P., Roberts, S.J., Gohl, K., Larter, R.D., Kuhn, G., 2017. West Antarctic Ice Sheet retreat driven by Holocene warm water incursions. Nature 547 (7661), 43–48. https://doi.org/10.1038/nature22995.

Hogan, K.A., Dowdeswell, J.A., Larter, R.D., Ó Cofaigh, C., Bartholemew, I., 2016. Subglacial meltwater channels in Marguerite Trough, western Antarctic Peninsula. In: Dowdeswell, J. A., Canals, M., Jakobsson, M., Todd, B. J., Dowdeswell, E. K., Hogan, K. A. (Eds.), Atlas of Submarine Glacial Landforms: Modern, Quaternary and Ancient. Geological Society, London, Memoirs 46, 215–216. https://doi.org/10.1144/M46.178.

Horgan, H.J., Anandakrishnan, S., Jacobel, R.W., Christianson, K., Alley, R.B., Heeszel, D.S., Picotti, S., Walter, J.I., 2012. Subglacial Lake Whillans—seismic observations of a shallow active reservoir beneath a West Antarctic ice stream. Earth Planet. Sci. Lett. 331, 201–209. https://doi.org/10.1016/j.epsl.2012.02.023.

Huuse, M., Lykke-Andersen, H., 2000. Overdeepened Quaternary valleys in the eastern Danish North Sea: morphology and origin. Quat. Sci. Rev. 19 (12), 1233–1253. https://doi.org/10.1016/S0277-3791(99)00103-1.

Jacobel, R.W., Scambos, T.A., Nereson, N.A., Raymond, C.F., 2000. Changes in the margin of Ice Stream C, Antarctica. J. Glaciol. 46 (152), 102–110. https://doi.org/10.3189/172756500781833485.

Jacobs, S.S., Hellmer, H.H., Jenkins, A., 1996. Antarctic ice sheet melting in the Southeast Pacific. Geophys. Res. Lett. 23 (9), 957–960. https://doi.org/10.1029/96GL00723.

Jakobsson, M., Anderson, J.B., Nitsche, F.O., Gyllencreutz, R., Kirshner, A.E., Kirchner, N., O'Regan, M., Mohammad, R., Eriksson, B., 2012. Ice sheet retreat dynamics inferred from glacial morphology of the central Pine Island Bay Trough. West Antarctica. Quaternary Science Reviews. 38, 1–10. https://doi.org/10.1016/j.quascirev.2011.12.017.

Jakobsson, M., Gyllencreutz, R., Mayer, L.A., Dowdeswell, J.A., Canals, M., Todd, B.J., Dowdeswell, E.K., Hogan, K.A., Larter, R.D., 2016. In: Dowdeswell, J. A., Canals, M., Jakobsson, M., Todd, B. J., Dowdeswell, E. K., Hogan, K. A. (Eds.), Atlas of Submarine Glacial Landforms: Modern, Quaternary and Ancient. Geological Society, London, Memoirs 46, 17–40. https://doi.org/10.1144/M46.182.

Jansen, J.D., Codilean, A.T., Stroeven, A.P., Fabel, D., Hättestrand, C., Kleman, J., Harbor, J.M., Heyman, J., Kubik, P.W., Xu, S., 2014. Inner gorges cut by subglacial meltwater during Fennoscandian ice sheet decay. Nat. Commun. 5, 3815. https://doi.org/10.1038/ncomms4815.

Jenkins, A., 2011. Convection-driven melting near the grounding lines of ice shelves and tidewater glaciers. J. Phys. Oceanogr. 41 (12), 2279–2294. https://doi.org/10.1175/JPO-D-11-03.1.

Jenkins, A., Vaughan, D.G., Jacobs, S.S., Hellmer, H.H., Keys, J.R., 1997. Glaciological and oceanographic evidence of high melt rates beneath Pine Island Glacier, West Antarctica. J. Glaciol. 43 (143), 114–121. https://doi.org/10.3189/S0022143000002872.

Jenkins, A., Dutrieux, P., Jacobs, S.S., McPhail, S.D., Perrett, J.R., Webb, A.T., White, D., 2010. Observations beneath Pine Island Glacier in West Antarctica and implications for its retreat. Nat. Geosci. 3, 468–472. https://doi.org/10.1038/ngeo890.

Johnson, N.L., Kotz, S., 1970. Distributions in Statistics: Continuous Univariate Distributions. Volume 1. Wiley, New York.

Jolliffe, I.T., 2002. Principal Component Analysis. Springer, New York.

Jordan, T.A., Ferraccioli, F., Corr, H., Graham, A., Armadillo, E., Bozzo, E., 2010. Hypothesis for mega-outburst flooding from a palaeo-subglacial lake beneath the East Antarctic Ice Sheet. Terra Nova 22 (4), 283–289. https://doi.org/10.1111/j.1365-3121.2010.00944.x.

Jørgensen, F., Sandersen, P.B., 2006. Buried and open tunnel valleys in Denmark—erosion beneath multiple ice sheets. Quat. Sci. Rev. 25 (11), 1339–1363. https://doi.org/10.1016/j.quascirev.2005.11.006.

Joughin, I., Tulaczyk, S., Bindschadler, R., Price, S.F., 2002. Changes in West Antarctic ice stream velocities: observation and analysis. Journal of Geophysical Research: Solid Earth. 107 (B11). https://doi.org/10.1029/2001JB001029.

Kapitsa, A.P., Ridley, J.K., de Q Robin, G., Siegert, M.J., Zotikov, I.A., 1996. A large deep freshwater lake beneath the ice of central East Antarctica. Nature. 381 (6584), 684. https://doi.org/10.1038/381684a0.

Kehew, A.E., Piotrowski, J.A., Jørgensen, F., 2012. Tunnel valleys: concepts and controversies—a review. Earth Sci. Rev. 113 (1–2), 33–58. https://doi.org/10.1016/j.earscirev.2012.02.002.

Kennedy, D.S., Anderson, J.B., 1989. Glacial-marine sedimentation and Quaternary glacial history of Marguerite Bay, Antarctic Peninsula. Quaternary Research 31, 255–276. https://doi.org/10.1016/0033-5894(89)90008-2.

King, E.C., Hindmarsh, R.C., Stokes, C.R., 2009. Formation of mega-scale glacial lineations observed beneath a West Antarctic ice stream. Nat. Geosci. 2 (8), 585–588. https://doi.org/10.1038/ngeo581.

Kingslake, J., Ely, J.C., Das, I., Bell, R.E., 2017. Widespread movement of meltwater onto and across Antarctic ice shelves. Nature. 544 (7650), 349–352. https://doi.org/10.1038/nature22049.

Kipf, A., Mortimer, N., Werner, R., Gohl, K., Van Den Bogaard, P., Hauff, F., Hoernle, K., 2012. Granitoids and dykes of the Pine Island Bay region, West Antarctica. Antarct. Sci. 24 (05), 473–484. https://doi.org/10.1017/S0954102012000259.

Kirkham, J.D., Hogan, K.A., Larter, R.D., Arnold, N.S., Nitsche, F.O., Golledge, N.R., Dowdeswell, J.A., 2019. Past water flow beneath Pine Island and Thwaites glaciers, West Antarctica. Cryosphere 13, 1959–1981. https://doi.org/10.5194/tc-13-1959-2019.

Kirshner, A.E., Anderson, J.B., Jakobsson, M., O'Regan, M., Majewski, W., Nitsche, F.O., 2012. Post-LGM deglaciation in Pine island Bay, West Antarctica. Quat. Sci. Rev. 38, 11–26. https://doi.org/10.1016/j.quascirev.2012.01.017.

Klages, J.P., Kuhn, G., Graham, A.G., Hillenbrand, C.D., Smith, J.A., Nitsche, F.O., Larter, R.D., Gohl, K., 2015. Palaeo-ice stream pathways and retreat style in the easternmost Amundsen Sea Embayment, West Antarctica, revealed by combined multibeam bathymetric and seismic data. Geomorphology 245, 207–222. https://doi.org/10.1016/j.geomorph.2015.05.020.

Kristensen, T.B., Huuse, M., Piotrowski, J.A., Clausen, O.R., 2007. A morphometric analysis of tunnel valleys in the eastern North Sea based on 3D seismic data. J. Quat. Sci. 22 (8), 801–815. https://doi.org/10.1002/jqs.1123.

Kristensen, T.B., Piotrowski, J.A., Huuse, M., Clausen, O.R., Hamberg, L., 2008. Time-transgressive tunnel valley formation indicated by infill sediment structure, North Sea—the role of glaciohydraulic supercooling. Earth Surf. Process. Landf. 33 (4), 546–559. https://doi.org/10.1002/esp.1668.

Kuhn, G., Hillenbrand, C.D., Kasten, S., Smith, J.A., Nitsche, F.O., Frederichs, T., Wiers, S., Ehrmann, W., Klages, J.P., Mogollón, J.M., 2017. Evidence for a palaeo-subglacial lake on the Antarctic continental shelf. Nat. Commun. 8, 15591. https://doi.org/10.1038/ncomms15591.

LaMasurier, W., 2013. Shield volcanoes of Marie Byrd Land, West Antarctic rift: oceanic island similarities, continental signature, and tectonic controls. Bull. Volcanol. 75, 726–744. https://doi.org/10.1007/s00445-013-0726-1.

Larsen, I.J., Lamb, M.P., 2016. Progressive incision of the Channeled Scablands by outburst floods. Nature. 538 (7624), 229–232. https://doi.org/10.1038/nature19817.

Larter, R.D., Barker, P.F., 1989. Seismic stratigraphy of the Antarctic Peninsula Pacific margin: a record of Pliocene–Pleistocene ice volume and paleoclimate. Geology. 17, 731–734. https://doi.org/10.1130/0091-7613(1989)0172.3.CO;2.

Larter, R.D., Cunningham, A.P., 1993. The depositional pattern and distribution of glacial–interglacial sequences on the Antarctic Peninsula Pacific margin. Mar. Geol. 109, 203–219. https://doi.org/10.1016/0025-3227(93)90061-Y.

Larter, R.D., Rebesco, M., Vanneste, L.E., Gamboa, L.A.P., Barker, P.F., 1997. Cenozoic tectonic, sedimentary and glacial history of the continental shelf west of Graham Land, Antarctic Peninsula. In: Barker, P.F., Cooper, A.K. (Eds.), Geology and Seismic Stratigraphy of the Antarctic Margin. 2, Washington. D.C, American Geophysical Union, pp. 1–27 https://doi.org/10.1029/AR071p0001.

Larter, R.D., Graham, A.G., Gohl, K., Kuhn, G., Hillenbrand, C.D., Smith, J.A., Deen, T.J., Livermore, R.A., Schenke, H.W., 2009. Subglacial bedforms reveal complex basal regime in a zone of paleo–ice stream convergence, Amundsen Sea embayment, West Antarctica. Geology. 37 (5), 411–414. https://doi.org/10.1130/G25505A.1.

Larter, R.D., Anderson, J.B., Graham, A.G., Gohl, K., Hillenbrand, C.D., Jakobsson, M., Johnson, J.S., Kuhn, G., Nitsche, F.O., Smith, J.A., Witus, A.E., 2014. Reconstruction of changes in the Amundsen Sea and Bellingshausen sea sector of the West Antarctic ice sheet since the last glacial maximum. Quat. Sci. Rev. 100, 55–86. https://doi.org/10.1016/j.quascirev.2013.10.016.

Larter, R.D., Hogan, K.A., Hillenbrand, C.-D., Smith, J.A., Batchelor, C.L., Cartigny, M., Tate, A. J., Kirkham, J.D., Roseby, Z., Kuhn, G., Graham, A.G.C., Dowdeswell, J.A., 2019. Subglacial hydrological control on flow of an Antarctic Peninsula palaeo-ice stream. Cryosphere 13, 1583–1596. https://doi.org/10.5194/tc-13-1583-2019.

Le Brocq, A.M., Payne, A.J., Siegert, M.J., Alley, R.B., 2009. A subglacial water-flow model for West Antarctica. J. Glaciol. 55 (193), 879–888. https://doi.org/10.3189/002214309790152564.

Le Brocq, A.M., Ross, N., Griggs, J.A., Bingham, R.G., Corr, H.F., Ferraccioli, F., Jenkins, A., Jordan, T.A., Payne, A.J., Rippin, D.M., Siegert, M.J., 2013. Evidence from ice shelves for channelized meltwater flow beneath the Antarctic Ice Sheet. Nat. Geosci. 6 (11), 945–948. https://doi.org/10.1038/ngeo1977.

Lewis, A.R., Marchant, D.R., Kowalewski, D.E., Baldwin, S.L., Webb, L.E., 2006. The age and origin of the Labyrinth, western Dry Valleys, Antarctica: evidence for extensive middle Miocene subglacial floods and freshwater discharge to the Southern Ocean. Geology. 34 (7), 513–516. https://doi.org/10.1130/G22145.1.

Lindeque, A., Gohl, K., Henrys, S., Wobbe, F., Davy, B., 2016. Seismic stratigraphy along the Amundsen Sea to Ross Sea continental rise: a cross-regional record of pre-glacial to glacial processes of the West Antarctic margin. Palaeogeogr. Palaeoclimatol. Palaeoecol. 443, 183–202. https://doi.org/10.1016/j.palaeo.2015.11.017.

Livingstone, SJ, Ó Cofaigh, C, Stokes, CR, Hillenbrand, CD, Vieli, A, Jamieson, SS, 2012. Antarctic palaeo-ice streams. Earth Sci. Rev. 111(1), 90–128. doi:https://doi.org/10.1016/j.earscirev.2011.10.003.

Livingstone, S.J., Ó Cofaigh, C., Stokes, C.R., Hillenbrand, C.D., Vieli, A., Jamieson, S.S., 2013. Glacial geomorphology of Marguerite Bay palaeo-ice stream, western Antarctic Peninsula. Journal of Maps. 9 (4), 558–572. https://doi.org/10.1080/17445647.2013.829411.

Loose, B., Naveira Garabato, A.C., Schlosser, P., Jenkins, W.J., Vaughan, D., Heywood, K.J., 2018. Evidence of an active volcanic heat beneath the Pine Island Glacier. Nat. Commun. 9, 2431. https://doi.org/10.1038/s41467-018-04421-3.

Lowe, A.L., Anderson, J.B., 2002. Reconstruction of the West Antarctic ice sheet in Pine Island Bay during the Last Glacial Maximum and its subsequent retreat history. Quat. Sci. Rev. 21 (16), 1879–1897. https://doi.org/10.1016/S0277-3791(02)00006-9.

Lowe, A.L., Anderson, J.B., 2003. Evidence for abundant subglacial meltwater beneath the paleo-ice sheet in Pine Island Bay, Antarctica. J. Glaciol. 49 (164), 125–138. https://doi.org/10.3189/172756503781830971.

MacRae, R.A., Christians, A.R., 2013. A reexamination of Pleistocene tunnel valley distribution on the central Scotian Shelf. Can. J. Earth Sci. 50 (5), 535–544. https://doi.org/10.1139/cjes-2012-0057.

Mandal, U.K., Warrington, D.N., Bhardwaj, A.K., Bar-Tal, A., Kautsky, L., Minz, D., Levy, G.J., 2008. Evaluating impact of irrigation water quality on a calcareous clay soil using principal component analysis. Geoderma. 144 (1), 189–197. https://doi.org/10.1016/j.geoderma.2007.11.014.

Mangold, N., Mangeney, A., Migeon, V., Ansan, V., Lucas, A., Baratoux, D., Bouchut, F., 2010. Sinuous gullies on Mars: frequency, distribution, and implications for flow properties. Journal of Geophysical Research: Planets. 115 (E11). https://doi.org/10.1029/2009JE003540.

Martos, Y.M., Catalán, M., Jordan, T.A., Golynsky, A., Golynsky, D., Eagles, G., Vaughan, D.G., 2017. Heat flux distribution of Antarctica unveiled. Geophys. Res. Lett. 44 (22), 11417–11426. https://doi.org/10.1002/2017GL075609.

Mayer, L.A., Paton, M., Gee, L., Gardner, S.V., Ware, C., 2000. Interactive 3-D Visualization: a tool for seafloor navigation, exploration and engineering. OCEANS 2000 MTS/IEEE Conference and Exhibition. Vol. 2. IEEE, pp. 913–919. https://doi.org/10.1109/OCEANS.2000.881373.

Meyer, C.R., Fernandes, M.C., Creyts, T.T., Rice, J.R., 2016. Effects of ice deformation on Röthlisberger channels and implications for transitions in subglacial hydrology. J. Glaciol. 62, 750–762. https://doi.org/10.1017/jog.2016.65.

Montelli, A., Gulick, S.P., Fernandez, R., Frederick, B.C., Shevenell, A.E., Leventer, A., Blankenship, D.D., 2019. Seismic stratigraphy of the Sabrina Coast shelf, East Antarctica: Early history of dynamic meltwater-rich glaciations. Geological Society of America Bulletin https://doi.org/10.1130/B35100.1.

Mugford, R.I., Dowdeswell, J.A., 2011. Modeling glacial meltwater plume dynamics and sedimentation in high-latitude fjords. Journal of Geophysical Research: Earth Surface. 116 (F1). https://doi.org/10.1029/2010JF001735.

Murray, T., Corr, H., Forieri, A., Smith, A.M., 2008. Contrasts in hydrology between regions of basal deformation and sliding beneath Rutford Ice Stream, West Antarctica, mapped using radar and seismic data. Geophys. Res. Lett. 35 (12). https://doi.org/10.1029/2008GL033681.

Ng, F.S., 2000. Canals under sediment-based ice sheets. Annals of Glaciology 30, 146–152. https://doi.org/10.3189/172756400781820633.

Nitsche, F.O., Jacobs, S.S., Larter, R.D., Gohl, K., 2007. Bathymetry of the Amundsen Sea continental shelf: Implications for geology, oceanography, and glaciology. Geochem. Geophys. Geosyst. 8 (10). https://doi.org/10.1029/2007GC001694.

Nitsche, F.O., Gohl, K., Larter, R.D., Hillenbrand, C.D., Kuhn, G., Smith, J.A., Jacobs, S., Anderson, J.B., Jakobsson, M., 2013. Paleo ice flow and subglacial meltwater dynamics in Pine Island Bay, West Antarctica. Cryosphere 7 (1), 249–262. https://doi.org/10.5194/tc-7-249-2013.

Nitsche, F.O., Larter, R.D., Gohl, K., Graham, A.G., Kuhn, G., 2016. Bedrock channels in Pine Island Bay, West Antarctica. In: Dowdeswell, J.A., Canals, M., Jakobsson, M., Todd, B.J., Dowdeswell, E.K., Hogan, K.A. (Eds.), Atlas of Submarine Glacial Landforms: Modern. Quaternary and Ancient. Geological Society of London, Memoirs, London, pp. 217–218 https://doi.org/10.1144/M46.1.

Noormets, R., Dowdeswell, J.A., Larter, R.D., Ó Cofaigh, C., Evans, J., 2009. Morphology of the upper continental slope in the Bellingshausen and Amundsen Seas—implications for sedimentary processes at the shelf edge of West Antarctica. Mar. Geol. 258 (1), 100–114. https://doi.org/10.1016/j.margeo.2008.11.011.

Nye, J.F., 1976. Water flow in glaciers: jökulhlaups, tunnels and veins. J. Glaciol. 17 (76), 181–207. https://doi.org/10.1017/S002214300001354X.

Ó Cofaigh, C., Pudsey, C.J., Dowdeswell, J.A., Morris, P., 2002. Evolution of subglacial bedforms along a paleo-ice stream, Antarctic Peninsula continental shelf. Geophys. Res. Lett. 29 (8). https://doi.org/10.1029/2001GL014488.

Ó Cofaigh, C., Dowdeswell, J.A., Allen, C.S., Hiemstra, J.F., Pudsey, C.J., Evans, J., Evans, D.J., 2005. Flow dynamics and till genesis associated with a marine-based Antarctic palaeo-ice stream. Quat. Sci. Rev. 24 (5), 709–740. https://doi.org/10.1016/j.quascirev.2004.10.006.

Ó Cofaigh, C., Dowdeswell, J.A., Evans, J., Larter, R.D., 2008. Geological constraints on Antarctic palaeo-ice-stream retreat. Earth Surf. Process. Landf. 33 (4), 513–525. https://doi.org/10.1002/esp.1669.

Ó Cofaigh, C., Davies, B.J., Livingstone, S.J., Smith, J.A., Johnson, J.S., Hocking, E.P., Hodgson, D.A., Anderson, J.B., Bentley, M.J., Canals, M., Domack, E., 2014. Reconstruction of ice-sheet changes in the Antarctic Peninsula since the Last Glacial Maximum. Quat. Sci. Rev. 100, 87–110. https://doi.org/10.1016/j.quascirev.2014.06.023.

Oswald, G.K.A., Robin, G.D.Q., 1973. Lakes beneath the Antarctic ice sheet. Nature. 245, 251–254. https://doi.org/10.1038/245251a0.

Ottesen, D., Dowdeswell, J.A., Rise, L., 2005. Submarine landforms and the reconstruction of fast-flowing ice streams within a large Quaternary ice sheet: the 2500-km-long Norwegian-Svalbard margin (57–80 N). Geol. Soc. Am. Bull. 117 (7–8), 1033–1050. https://doi.org/10.1130/B25577.1.

Ottesen, D., Dowdeswell, J.A., Landvik, J.Y., Mienert, J., 2007. Dynamics of the Late Weichselian ice sheet on Svalbard inferred from high-resolution sea-floor morphology. Boreas. 36 (3), 286–306. https://doi.org/10.1111/j.1502-3885.2007.tb01251.x.

Passchier, S., Laban, C., Mesdag, C.S., Rijsdijk, K.F., 2010. Subglacial bed conditions during Late Pleistocene glaciations and their impact on ice dynamics in the southern North Sea. Boreas. 39 (3), 633–647. https://doi.org/10.1111/j.1502-3885.2009.00138.x.

Patton, H., Swift, D.A., Clark, C.D., Livingstone, S.J., Cook, S.J., 2016. Distribution and characteristics of overdeepenings beneath the Greenland and Antarctic ice sheets: implications for overdeepening origin and evolution. Quat. Sci. Rev. 148, 128–145. https://doi.org/10.1016/j.quascirev.2016.07.012.

Pattyn, F., 2010. Antarctic subglacial conditions inferred from a hybrid ice sheet/ice stream model. Earth Planet. Sci. Lett. 295 (3–4), 451–461. https://doi.org/10.1016/j.epsl.2010.04.025.

Pattyn, F., Van Huele, W., 1998. Power law or power flaw? Earth Surf. Process. Landf. 23 (8), 761–767. https://doi.org/10.1002/(SICI)1096-9837(199808).

Perol, T., Rice, J.R., Platt, J.D., Suckale, J., 2015. Subglacial hydrology and ice stream margin locations. Journal of Geophysical Research: Earth Surface. 120, 1352–1368. https://doi.org/10.1002/2015JF003542.

Peters, L.E., Anandakrishnan, S., Alley, R.B., Winberry, J.P., Voigt, D.E., Smith, A.M., Morse, D.L., 2006. Subglacial sediments as a control on the onset and location of two Siple Coast ice streams, West Antarctica. Journal of Geophysical Research: Solid Earth. 111 (B1). https://doi.org/10.1029/2005JB003766.

Piotrowski, J.A., 1997. Subglacial hydrology in north-western Germany during the last glaciation: groundwater flow, tunnel valleys and hydrological cycles. Quat. Sci. Rev. 16 (2), 169–185. https://doi.org/10.1016/S0277-3791(96)00046-7.

Pope, A., Rees, W.G., 2014. Impact of spatial, spectral, and radiometric properties of multispectral imagers on glacier surface classification. Remote Sens. Environ. 141, 1–13. https://doi.org/10.1016/j.rse.2013.08.028.

Powell, R.D., 1990. Glacimarine processes at grounding-line fans and their growth to ice-contact deltas. In: Dowdeswell, J.A., Scourse, J.D. (Eds), Glacimarine Environments: Processes and Sediments. Geol. Soc. Lond., Spec. Publ. 53, 53–73. https://doi.org/10.1144/GSL.SP.1990.053.01.03.

Praeg, D., 2003. Seismic imaging of mid-Pleistocene tunnel-valleys in the North Sea Basin—high resolution from low frequencies. J. Appl. Geophys. 53 (4), 273–298. https://doi.org/10.1016/j.jappgeo.2003.08.001.

Prothro, L.O., Simkins, L.M., Majewski, W., Anderson, J.B., 2018. Glacial retreat patterns and processes determined from integrated sedimentology and geomorphology records. Mar. Geol. 395, 104–119. https://doi.org/10.1016/j.margeo.2017.09.012.

Pugin, A.J.M., Oldenborger, G.A., Cummings, D.I., Russell, H.A., Sharpe, D.R., 2014. Architecture of buried valleys in glaciated Canadian Prairie regions based on high resolution geophysical data. Quat. Sci. Rev. 86, 13–23. https://doi.org/10.1016/j.quascirev.2013.12.007.

Rackebrandt, N., 2006. Mapping of the PARASOUND Penetration Depth in the Pine Island Bay. Term Paper, Master of Science Marine Geosciences, Department of Geosciences, University of Bremen, Germany, West Antarctica (22 pp.).

Ravier, E., Buoncristiani, J.F., Menzies, J., Guiraud, M., Clerc, S., Portier, E., 2015. Does porewater or meltwater control tunnel valley genesis? Case studies from the Hirnantian of Morocco. Palaeogeogr. Palaeoclimatol. Palaeoecol. 418, 359–376. https://doi.org/10.1016/j.palaeo.2014.12.003.

Rebesco, M., Camerlenghi, A., De Santis, L., Domack, E., Kirby, M., 1998. Seismic stratigraphy of Palmer Deep: a fault-bounded late Quaternary sediment trap on the inner continental shelf, Antarctic Peninsula Pacific margin. Mar. Geol. 151 (1), 89–110. https://doi.org/10.1016/S0025-3227(98)00057-7.

Rignot, E., Mouginot, J., Scheuchl, B., van den Broeke, M., van Wessem, M.J., Morlighem, M., 2019. Four decades of Antarctic Ice Sheet mass balance from 1979–2017. Proc. Natl. Acad. Sci. 116 (4), 1095–1103. https://doi.org/10.1073/pnas.1812883116.

Ringnér, M., 2008. What is principal component analysis? Nat. Biotechnol. 26 (3), 303. https://doi.org/10.1038/nbt0308-303.

Roberts, M.J., 2005. Jökulhlaups: a reassessment of floodwater flow through glaciers. Rev. Geophys. 43 (1). https://doi.org/10.1029/2003RG000147.

Robin, G.D.Q., Swithinbank, C.W.M., Smith, B.M.E., 1970. Radio echo exploration of the Antarctic ice sheet. International Symposium on Antarctic Glaciological Exploration (ISAGE), Hanover, New Hampshire, USA, 3–7 September.

Rose, K.C., Ross, N., Bingham, R.G., Corr, H.F., Ferraccioli, F., Jordan, T.A., Le Brocq, A.M., Rippin, D.M., Siegert, M.J., 2014. A temperate former West Antarctic ice sheet suggested by an extensive zone of subglacial meltwater channels. Geology. 42 (11), 971–974. https://doi.org/10.1130/G35980.1.

Sandersen, P.B., Jørgensen, F., Larsen, N.K., Westergaard, J.H., Auken, E., 2009. Rapid tunnel-valley formation beneath the receding Late Weichselian ice sheet in Vendsyssel, Denmark. Boreas. 38 (4), 834–851. https://doi.org/10.1111/j.1502-3885.2009.00105.x.

Sawagaki, T., Hirakawa, K., 1997. Erosion of bedrock by subglacial meltwater, Soya Coast, East Antarctica. Geografiska Annaler: Series A, Physical Geography. 79 (4), 223–238. https://doi.org/10.1111/1468-0459.00019.

Schenke, H.W., Gauger, S., Lemenkova, P., Feigl, T., 2008. Swath sonar bathymetry during POLARSTERN cruise ANT-XXIII/4 (PS69) with links to multibeam raw data files. Alfred Wegener Institute, Helmholtz Centre for Polar and Marine Research, Bremerhaven, PANGAEA https://doi.org/10.1594/PANGAEA.680792.

Scheuer, C., Gohl, K., Larter, R.D., Rebesco, M., Udintsev, G., 2006. Variability in Cenozoic sedimentation along the continental rise of the Bellingshausen Sea, West Antarctica. Mar. Geol. 227 (3–4), 279–298. https://doi.org/10.1016/j.margeo.2005.12.007.

Schoof, C., 2010. Ice-sheet acceleration driven by melt supply variability. Nature. 468 (7325), 803–806. https://doi.org/10.1038/nature09618.

Schroeder, D.M., Blankenship, D.D., Young, D.A., 2013. Evidence for a water system transition beneath Thwaites Glacier, West Antarctica. Proc. Natl. Acad. Sci. U. S. A. 110, 12225–12228. https://doi.org/10.1073/pnas.1302828110.

Schroeder, D.M., Blankenship, D.D., Young, D.A., Quartini, E., 2014. Evidence for elevated and spatially variable geothermal flux beneath the West Antarctic Ice Sheet. Proc. Natl. Acad. Sci. U. S. A. 111 (25), 9070–9072. https://doi.org/10.1073/pnas.1405184111.

Shapiro, N.M., Ritzwoller, M.H., 2004. Inferring surface heat flux distributions guided by a global seismic model: particular application to Antarctica. Earth Planet. Sci. Lett. 223 (1), 213–224. https://doi.org/10.1016/j.epsl.2004.04.011.

Shoemaker, E.M., 1991. On the formation of large subglacial lakes. Can. J. Earth Sci. 28 (12), 1975–1981. https://doi.org/10.1139/e91-179.

Shreve, R.L., 1972. Movement of water in glaciers. J. Glaciol. 11 (62), 205–214. https://doi.org/10.1017/S002214300002219X.

Shreve, R.L., 1985. Esker characteristics in terms of glacier physics, Katahdin esker system, Maine. Geol. Soc. Am. Bull. 96 (5), 639–646. https://doi.org/10.1130/0016-7606.

Siegert, M.J., Bamber, J.L., 2000. Subglacial water at the heads of Antarctic ice-stream tributaries. J. Glaciol. 46, 702–703.

Siegert, M.J., Dowdeswell, J.A., Gorman, M.R., McIntyre, N.F., 1996. An inventory of Antarctic sub-glacial lakes. Antarct. Sci. 8 (3), 281–286. https://doi.org/10.1017/S0954102096000405.

Siegert, M.J., Carter, S., Tabacco, I., Popov, S., Blankenship, D.D., 2005. A revised inventory of Antarctic subglacial lakes. Antarct. Sci. 17 (03), 453–460. https://doi.org/10.1017/S0954102005002889.

Siegert, M.J., Ross, N., Corr, H.F.J., Smith, B., Jordan, T.A., Bingham, R.G., Ferraccioli, F., Rippin, D.M., Le Brocq, A.M., 2014. Boundary conditions of an active West Antarctic subglacial lake: implications for storage of water beneath the ice sheet. Cryosphere 8, 15–24. https://doi.org/10.5194/tc-8-15-2014.

Siegert, M.J., Ross, N., Le Brocq, A.M., 2016. Recent advances in understanding Antarctic subglacial lakes and hydrology. Phil. Trans. R. Soc. A 374 (2059). https://doi.org/10.1098/rsta.2014.0306.

Simkins, L.M., Anderson, J.B., Greenwood, S.L., Gonnermann, H.M., Prothro, L.O., Halberstadt, A.R.W., Stearns, L.A., Pollard, D., DeConto, R.M., 2017. Anatomy of a meltwater drainage system beneath the ancestral East Antarctic ice sheet. Nat. Geosci. 10 (9), 691–697. https://doi.org/10.1038/ngeo3012.

Smith, B.E., Fricker, H.A., Joughin, I.R., Tulaczyk, S., 2009a. An inventory of active subglacial lakes in Antarctica detected by ICESat (2003–2008). J. Glaciol. 55 (192), 573–595. https://doi.org/10.3189/002214309789470879.

Smith, J.A., Hillenbrand, C.D., Larter, R.D., Graham, A.G., Kuhn, G., 2009b. The sediment infill of subglacial meltwater channels on the West Antarctic continental shelf. Quat. Res. 71 (2), 190–200. https://doi.org/10.1016/j.yqres.2008.11.005.

Smith, A.M., Woodward, J., Ross, N., Bentley, M.J., Hodgson, D.A., Siegert, M.J., King, E.C., 2018. Evidence for the long-term sedimentary environment in an Antarctic subglacial lake. Earth Planet. Sci. Lett. 504, 139–151. https://doi.org/10.1016/j.epsl.2018.10.011.

Stearns, L.A., Smith, B.E., Hamilton, G.S., 2008. Increased flow speed on a large East Antarctic outlet glacier caused by subglacial floods. Nat. Geosci. 1 (12), 827–831. https://doi.org/10.1038/ngeo356.

Stewart, M.A., Lonergan, L., 2011. Seven glacial cycles in the middle-late Pleistocene of northwest Europe: geomorphic evidence from buried tunnel valleys. Geology. 39 (3), 283–286. https://doi.org/10.1130/G31631.1.

Stewart, M.A., Lonergan, L., Hampson, G., 2013. 3D seismic analysis of buried tunnel valleys in the central North Sea: morphology, cross-cutting generations and glacial history. Quat. Sci. Rev. 72, 1–17. https://doi.org/10.1016/j.quascirev.2013.03.016.

Stokes, C.R., Clark, C.D., 2002. Are long subglacial bedforms indicative of fast ice flow? Boreas. 31 (3), 239–249. https://doi.org/10.1080/030094802760260355.

Sugden, D.E., Denton, G.H., Marchant, D.R., 1991. Subglacial meltwater channel systems and ice sheet overriding, Asgard Range, Antarctica. Geografiska Annaler. Series A. Physical Geography, 109–121 https://doi.org/10.2307/520986.

Sugden, D.E., Summerfield, M.A., Denton, G.H., Wilch, T.I., McIntosh, W.C., Marchant, D.R., Rutford, R.H., 1999. Landscape development in the Royal Society Range, southern Victoria Land, Antarctica: stability since the mid-Miocene. Geomorphology. 28 (3), 181–200. https://doi.org/10.1016/S0169-555X(98)00108-1.

Trusel, L.D., Frey, K.E., Das, S.B., Munneke, P.K., Broeke, M.R., 2013. Satellite-based estimates of Antarctic surface meltwater fluxes. Geophys. Res. Lett. 40 (23), 6148–6153. https://doi.org/10.1002/2013GL058138.

Tulaczyk, S., Kamb, W.B., Engelhardt, H.F., 2000. Basal mechanics of ice stream B, West Antarctica: 1. Till mechanics. Journal of Geophysical Research: Solid Earth. 105 (B1), 463–481. https://doi.org/10.1029/1999JB900329.

U.S. Geological Survey, 2007. Landsat Image Mosaic of Antarctica (LIMA), U.S. Geological Survey Fact Sheet 2007–3116, (4 pp.).

van der Vegt, P., Janszen, A., Moscariello, A., 2012. Tunnel valleys: current knowledge and future perspectives. Geol. Soc. Lond., Spec. Publ. 368 (1), 75–97. https://doi.org/10.1144/SP368.13.

van Dijke, J.J., Veldkamp, A., 1996. Climate-controlled glacial erosion in the unconsolidated sediments of northwestern Europe, based on a genetic model for tunnel valley formation. Earth Surf. Process. Landf. 21 (4), 327–340. https://doi.org/10.1002/(SICI)1096-9837(199604)21:4<327::AID-ESP540>3.0.CO;2-P.

Vargo, E., Pasupathy, R., Leemis, L.M., 2010. Moment-ratio diagrams for univariate distributions. J. Qual. Technol. 42, 276–286. https://doi.org/10.1007/978-3-319-43317-2_12.

Walder, J.S., Fowler, A., 1994. Channelized subglacial drainage over a deformable bed. J. Glaciol. 40 (134), 3–15. https://doi.org/10.1017/S0022143000003750.

Wei, W., Blankenship, D.D., Greenbaum, J.S., Gourmelen, N., Dow, C.F., Richter, T.G., Greene, C.A., Young, D.A., Lee, S., Kim, T.-W., Lee, W.S., Assmann, K.M., 2020. Getz Ice Shelf melt enhanced by freshwater discharge from beneath the West Antarctic Ice Sheet. Cryosphere 14, 1399–1408. https://doi.org/10.5194/tc-14-1399-2020.

Wellner, J.S., Heroy, D.C., Anderson, J.B., 2006. The death mask of the Antarctic ice sheet: comparison of glacial geomorphic features across the continental shelf. Geomorphology. 75 (1), 157–171. https://doi.org/10.1016/j.geomorph.2005.05.015.

Willis, I.C., Pope, E.L., Gwendolyn, J.M., Arnold, N.S., Long, S., 2016. Drainage networks, lakes and water fluxes beneath the Antarctic ice sheet. Ann. Glaciol. 57 (72), 1–13. https://doi.org/10.1017/aog.2016.15.

Wingham, D.J., Siegert, M.J., Shepherd, A., Muir, A.S., 2006. Rapid discharge connects Antarctic subglacial lakes. Nature. 440 (7087), 1033–1036. https://doi.org/10.1038/nature04660.

Witus, A.E., Branecky, C.M., Anderson, J.B., Szczucinski, W., Schroeder, D.M., Blankenship, D.D., Jakobsson, M., 2014. Meltwater intensive retreat in polar environments and investigation of associated sediments: example from Pine Island Bay. West Antarctica. Quaternary Science Reviews. 85, 99–118. https://doi.org/10.1016/j.quascirev.2013.11.021.

Wright, A., Siegert, M.J., 2011. The identification and physiographical setting of Antarctic subglacial lakes: an update based on recent discoveries. Geophysical Monograph Series. 192, 9–26. https://doi.org/10.1029/2010GM000933.
Wright, A., Siegert, M.J., 2012. A fourth inventory of Antarctic subglacial lakes. Antarct. Sci. 24 (06), 659–664. https://doi.org/10.1017/S095410201200048X.
Zwally, H.J., Abdalati, W., Herring, T., Larson, K., Saba, J., Steffen, K., 2002. Surface melt-induced acceleration of Greenland ice-sheet flow. Science. 297 (5579), 218–222. https://doi.org/10.1126/science.1072708.